I. MAGNETIC RESONANCE STUDIES OF PARAMAGNETIC SOLUTIONS

II. KINETICS OF THE FERROUS IRON-OXYGEN REACTION IN ACIDIC PHOSPHATE-PYROPHOSPHATE SOLUTIONS

Thesis by

James King, Jr.

In Partial Fulfillment of the Requirements

For the Degree of

Doctor of Philosophy

California Institute of Technology

Pasadena, California

1958

ACKNOWLEDGEMENT

It is with a deep sense of gratitude that I acknowledge the aid which my research advisors, Dr. N. Davidson and Dr. H. McConnell, have given me during my profitable years of graduate study at the California Institute of Technology. I am thankful for the opportunity to have worked with men of such high scholastic caliber and enjoy their friendship. I am especially grateful to Dr. N. Davidson for his continuous efforts to cultivate my scientific abilities and increase my understanding of the complex problems of science.

I wish to thank the General Education Board, the Danforth Foundation, and the California Institute of Technology for financial assistance during my graduate study. All the research in this thesis was financed by the Atomic Energy Commission.

The help and friendliness of all the members of the Caltech community have made the past years both pleasant and enjoyable.

I acknowledge, with pride, the patience and understanding shown by my wife, Jean, who was willing to make great sacrifices so that this work could be completed.

ABSTRACT

The techniques of Nuclear Magnetic Resonance and Electron Paramagnetic Resonance have been used to study the interaction of electrons and nuclei in solution. Results of a study of the interaction between paramagnetic manganeous ions (Mn^{++}) and water molecules indicate that the abnormally large ratio of the proton relaxation times, T_1/T_2, previously found in the system, can be essentially explained by an isotropic hyperfine interaction between the electrons and protons in the solution. When this interaction is destroyed by complexing the Mn^{++} with the hexadentate ligand, ethylenediaminetetraacetate (MnY^{-2}), or with the tetradentate ligand, nitrilotriacetate (MnX^{-1}), T_1 is increased slightly and T_2 is increased markedly, so that $T_1 \approx T_2$ and the ratio is unity as expected.

An isotropic hyperfine interaction is also found to exist in ferric fluoride solutions. The interaction between the electrons of the ferric ion and the fluoride nuclei produces characteristic resonance spectra for the different complexes in the system. From a study of the system, the existence in solution of the $FeF_6^{\equiv}$ complex is definitely established. A value for the dissociation constant of the complex is obtained and an upper limit is set for the rate of exchange of complexed and uncomplexed fluorides in the system. The amount of 2s - character of the Fe^{+++} — F^- bond in the ferric fluoride complexes is also obtained.

The shifts, due to the magnetic susceptibility in the system are treated in Section IV. It is found that the shifts deviate from the values one would expect if the susceptibility in the system were

isotropic. Both organic and inorganic systems are treated. The method used to measure these small shifts is also described.

Part II consists of a published article on the oxygenation of ferrous ion in acidic phosphate-pyrophosphate solutions.

TABLE OF CONTENTS

TABLE OF CONTENTS (Cont'd)

I. INTRODUCTION

The techniques of Electron Paramagnetic Resonance (EPR) and Nuclear Magnetic Resonance (NMR) have found extensive use in the fields of chemistry and chemical physics since their discoveries in 1945 and 1946. The methods have been used to yield information about molecular structure, distribution of electrons in atoms and molecules, and the rates of fast chemical reactions. In these studies the magnetic resonance observation of the electron or nucleus provides information about the electronic structure and exchange properties of the system without significantly perturbing the system.

The investigations presented in this thesis are concerned only with the application of (NMR) and (EPR) to the study of species in liquid solutions. There shall not be an attempt to present the complete theories of (NMR) and (EPR) since these are treated quite adequately in a number of books (1), (2), (3) and review articles (4), (5), (6), (7). Only the theory necessary to understand the experimental results will be presented.

Since both EPR and NMR are spectroscopic in nature, the equation serving as their foundation is the fundamental equation of spectroscopy.

$$h\underline{\nu} = E_1 - E_2 = \underline{\Delta E} \tag{1}$$

where the symbols have their usual meanings.

The nuclear resonance condition is derived from this equation by considering an ensemble of nuclei, each with angular momentum $\underline{I}$

and magnetic moment $\underline{\mu}$, in a magnetic field $\underline{H}$. In such a field there arises a set of $2I+1$ quantized Zeeman energy levels due to the different orientations of the nuclei. The populationsof the levels vary according to a Boltzmann distribution, which at normal temperatures and magnetic fields of a few thousand gauss, results in a slight excess population in the lower levels. Transitionsbetween the levels can be induced by application of a small oscillating field, H_1, generated by a radiofrequency coil at right angles to a larger static field, H_o . The energy of the Zeeman levels is given by the expression

$$\underline{E} = - \underline{\mu} \cdot \underline{H} = - \mu H \cos \theta \qquad (2)$$

The angle θ between the magnetic moment vector and the magnetic field vector is defined by the relation, $\cos \theta = m/I$ where m is the magnetic quantum number running from $-I$ to $+I$. Transitions are permitted for which $\Delta m = \pm 1$. Thus,

$$\underline{\Delta E} = h \underline{\nu} = \underline{\mu} \underline{H}/I \qquad (3)$$

This nuclear resonance condition is usually expressed in terms of an angular frequency, $\underline{\omega}$, equal to $2\pi \underline{\nu}$. When this substitution is made, equation 3 becomes

$$\underline{\omega} = 2\pi \underline{\mu} \underline{H}/Ih = \underline{\mu} \underline{H}/Ih = \gamma \underline{H} \qquad (4)$$

The quantity γ is called the gyromagnetic ratio. The angular frequency

$\underline{\omega}$ is the well known Larmor precession frequency of the nuclear magnetic moment vector, $\underline{\mu}$, about the magnetic field vector $\underline{H}$. At resonance this frequency must be equal to the externally applied radiofrequency. In liquids, as will be seen later, $\underline{H}$ in equation 4, is not necessarily equal to the externally applied magnetic field. Two different, but related, methods of investigating the nuclear resonance phenomenon have been developed by Bloch (8) and Purcell (9).

The condition necessary to observe electron magnetic resonance is similar to that for nuclear resonance, differing only in the magnetic properties of the electron as compared to those of the nucleus. The energy of interaction between an electron, with angular momentum $1/2\ \hbar$ and magnetic moment $\mu_\beta = \frac{e\hbar}{2mc}$, and a magnetic field $\underline{H}$ is also given by

$$E = -\underline{\mu} \cdot \underline{H} \tag{2}$$

This interaction is at a minimum when $\underline{\mu}$ is parallel to the direction of $\underline{H}$. For an electron spin the separation of the energy levels in a field $\underline{H}$ is

$$\Delta E = 2\ \mu_z\ \underline{H} = g\mu_\beta \underline{H} \tag{5}$$

where $\underline{g}$, the "spectroscopic splitting factor" would be equal to 2.0 if the electron were completely free. In practice the g-value differs from 2.0 because the electron is affected by the binding forces in the molecule. Combining equations 1 and 5 the condition for electron magnetic resonance is obtained.

$$h\underline{\nu} = g\mu_\beta \underline{H} \qquad (6)$$

The electron resonance is usually written as above to distinguish it from the nuclear case (equation 4). However, if $\underline{\omega}/2\pi$ is substituted for ν in equation 6 an expression quite similar to equation 4 is obtained; the difference being only between the value for the magnetic properties of the nucleus as compared to those of the electron. This difference also accounts for the fact that (NMR) is observed in the radiofrequency range (1 - 40 Mc) while EPR occurs in the microwave region (1 - 300 KMc).

The advent of NMR and EPR made available, for the first time, a method for studying experimentally the interaction between the electrons and nuclei in solution.

II. PROTON RELAXATION IN MN^{++} SOLUTIONS

The properties of the nucleus first found to be dependent on the presence of paramagnetic ions in solution were the relaxation times. In the original treatment of the problem by Bloembergen, Purcell and Pound (10), the paramagnetic species were assumed to affect the relaxation times through a dipole-dipole interaction. As pointed out by the above investigators, the use of such an interaction leads to the prediction that the relaxation times should be approximately equal at the frequencies normally used in NMR experiments (30 - 40 Mc). This relation was approximately verified by Bloembergen, Purcell and Pound and has been rather accurately verified in later works. However, Zimmerman (11), in measuring the proton relaxation times in a number of paramagnetic solutions, made the significant discovery that in aqueous manganese (Mn^{++}) solutions (either MnSO4 or $MnCl_2$) the times were not equal but differed by a factor of 10.

This section deals with the theories advanced to explain this unique behavior of the proton relaxation times in aqueous manganese solutions and the results of experiments designed to test the proposed theories. Before presenting the proposed explanations, the well known classical definitions of the relaxation times are discussed.

Theory

The relaxation times determine the speed with which the total magnetization in the system returns to its equilibrium value after being

changed by the oscillating magnetic field. The equation expressing this change in $\underline{M}$ is given by

$$\frac{d\underline{M}}{dt} = \gamma \underline{M} \times \underline{H} \tag{7}$$

where $\underline{H}$ is the total magnetic field acting in the system.

The steady-state solution of equation 7 for constant $\underline{H}$ represents the precession of the vector $\underline{M}$ about $\underline{H}$ with angular frequency $\gamma \underline{H}$. However, in actual nuclear resonance experiments $\underline{H}$ is not constant but has components

$$H_x = H_1 \cos\omega t \qquad H_y = -H_1 \sin\omega t \qquad H_z = H_o \tag{8}$$

The components H_x and H_y represent a magnetic field of amplitude H_1, rotating in a plane normal to the large static field H_o.

There are other mechanisms, not given by equation 7 which cause a change in the magnetization. These lead to a definition of the relaxation times. If the amplitude, H_1, of the oscillating magnetic field is reduced to zero, the z-component of the magnetization will approach the equilibrium value of the total magnetization, $\underline{M}_o$, exponentially. The characteristic time describing the approach to equilibrium is defined as $\underline{T}_1$, the longitudinal relaxation time. Thus

$$\frac{dM_z}{dt} = \frac{M_o - M_z}{\underline{T}_1} \tag{9}$$

The transverse components M_x and M_y represent the rotating components of the precessing magnetization $\underline{M}$. The exponential approach to their equilibrium value, zero, is governed by the transverse relaxation time $\underline{T}_2$.

$$\frac{dM_x}{dt} = -\frac{M_x}{\underline{T}_2} \qquad \frac{dM_y}{dt} = -\frac{M_y}{\underline{T}_2} \tag{10}$$

Although the relaxation times are defined for the case of no externally applied oscillating magnetic field, there still exists local fluctuating magnetic fields in the system due to the interaction between the nuclei themselves. These fluctuations are responsible for the decay of the magnetization. Since the transverse components are rotating they are not influenced by the same frequencies from the fluctuating magnetic fields as is the logitudinal component. The importance of this difference will manifest itself in subsequent discussion.

As mentioned before, Bloembergen, Purcell and Pound (10) studied the effects of dissolved paramagnetic ions on the relaxation times of protons in aqueous solutions. In a theoretical treatment of the problem, they assumed that the paramagnetic ions affected the relaxation times through a dipole-dipole interaction between the proton spins and the electron spins of the paramagnetic species. This type of interaction is dependent on the random motion in the system since it is a function of the angle between the dipole moment vectors. This angle is constantly changing due to the Brownian motion in the system. Accordingly, to describe this motion the above investigators defined

a correlation time τ_c which can be thought of, in some cases, as the time it takes a molecule to make a complete revolution or the time it takes one molecule to diffuse by another. The tumbling time, τ_c , is approximately 10^{-11} sec. At frequencies normally used in NMR experiments (30 - 40 Mc) this time is much shorter than the period of rotation of the transverse components M_x and M_y since these precess with the Larmor frequency $\underline{\omega}$. Under these conditions $\underline{T}_1$ and $\underline{T}_2$ should be equal, since the rotation of the transverse components is unimportant.

Solomon (12), by assuming a dipole-dipole type interaction between a nucleus and a paramagnetic ion in solution derived a set of equations which predict the near equality of $\underline{T}_1$ and $\underline{T}_2$ in the frequency range 30 - 40 Mc. These equations are

$$\left(\frac{1}{\underline{T}_1}\right)_{dp} = \frac{h^2 \gamma_I^2 \gamma_S^2}{10 r^6}\left[\frac{\underline{\tau}_c}{1+(\underline{\omega}_I - \underline{\omega}_S)^2 \underline{\tau}_c^2} + \frac{3\underline{\tau}_c}{1+\underline{\omega}_I^2 \underline{\tau}_c^2} + \frac{6\underline{\tau}_c}{1+(\underline{\omega}_i+\underline{\omega}_S)^2 \underline{\tau}_c^2}\right] \quad (11)$$

$$\left(\frac{1}{\underline{T}_2}\right)_{dp} = \frac{h^2 \gamma_I^2 \gamma_S^2}{20 r^6}\left[\frac{\underline{\tau}_c}{1+(\underline{\omega}_I - \underline{\omega}_S)^2 \underline{\tau}_c^2} + \frac{3\underline{\tau}_c}{1+\underline{\omega}_I^2 \underline{\tau}_c^2} + \frac{6\underline{\tau}_c}{1+\underline{\omega}_S^2 \underline{\tau}_c^2} + \frac{6\underline{\tau}_c}{1+(\underline{\omega}_I+\underline{\omega}_S)^2 \underline{\tau}_c^2}\right] \quad (12)$$

γ_I, the gyromagnetic ratio of the protons with Larmor precession frequency $\underline{\omega}_I$, is equal to 2.66×10^4 radius sec^{-1} $gauss^{-1}$. The gyromagnetic ratio of the electrons, γ_S , with frequency $\underline{\omega}_S$ is equal to 1.8×10^7 radians sec^{-1} $gauss^{-1}$. Under the conditions normally used

in NMR experiments ($H_o \sim$ 10,000 gauss, ν = 30 - 40 Mc), $\underline{\omega}_I = 2 \times 10^8$ radians sec^{-1} and $\underline{\omega}_S = 1 \times 10^{11}$ radians sec^{-1}. Therefore, $\underline{\omega}_I \underline{\tau}_c << \underline{\omega}_S \underline{\tau}_c < 1$. When these conditions are satisfied, equations 11 and 12 predict that $\underline{T}_1$ and $\underline{T}_2$ should be approximately equal. This near equality of the relaxation times was found by Solomon to exist for protons in aqueous solutions of ferric (Fe^{+++}) ions at 30 Mc.

It has since been shown by Nolle and Morgan (13) that $\underline{T}_1$ and $\underline{T}_2$ are also approximately equal for protons in aqueous solutions containing cobaltous (Co^{++}) and neodymium (Nd^{+++}) ions.

It, therefore, appears from the work of Zimmerman (11) that only in aqueous solutions of Mn^{++} are the relaxation times not approximately equal at 30 Mc.

This abnormal $\underline{T}_1/\underline{T}_2$ ratio in Mn^{++} solutions was further studied by Nolle and Morgan (13) and by Bloom (14). The former authors found that $\underline{NT}_2$ (N = concentrations in mole $liter^{-1}$) is constant at the value 1.5×10^{-5} sec. mole $liter^{-1}$ from 2.7 to 28.7 Mc whereas $\underline{NT}_1$ increased from 3.2×10^{-5} sec mole $liter^{-1}$ at 2.7 Mc to 1.0×10^{-4} sec at 28.7 Mc. Bloom reports that $\underline{T}_1$ and $\underline{T}_2$ are equal at low frequency (2200 cps) with $\underline{NT} = 1.5 \times 10^{-5}$. However, $\underline{T}_1$ increases between 10^4 and 10^6 cps to the value $\underline{NT}_1 = 3 \times 10^{-5}$. Thus, it appears that $\underline{T}_2$ is frequency independent, whereas $\underline{T}_1$ as a function of frequency has plateaus between 10^3 and 10^4 cps and 5×10^5 to 5×10^6 cps, but decreases by a factor of three around 7×10^4 cps and is decreasing again at 10^7 cps. This situation is illustrated in figure 1.

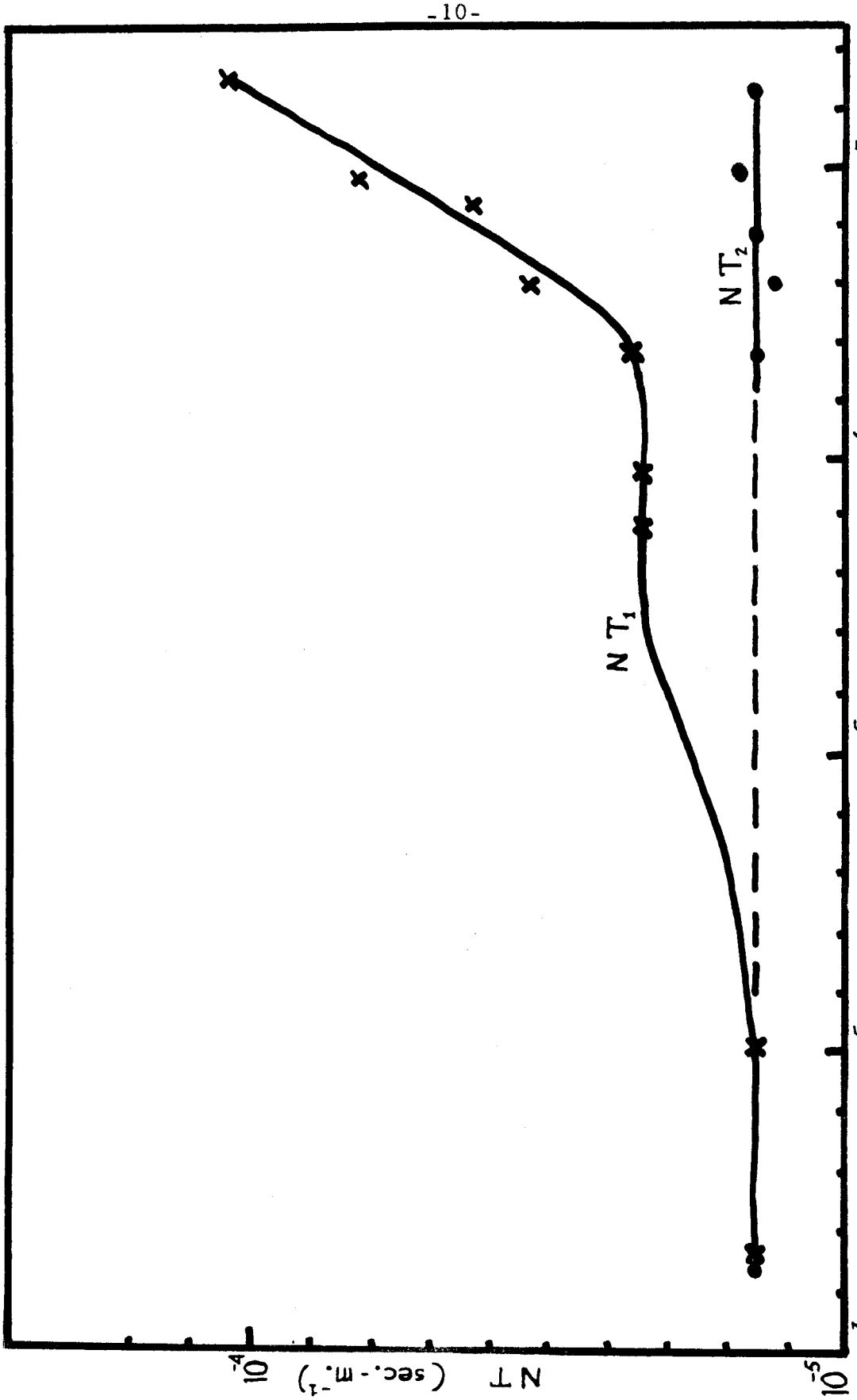

Fig. 1

Relaxation Times as a Function of Frequency

If one assumes that τ_c in equations 11 and 12 is approximately 10^{-11} sec, these equations do not explain the above phenomena. There were attempts by Bloom and by Nolle and Morgan to modify these equations by assuming that the correct correlation time to be used is not τ_c, the tumbling time, but a longer time based on the chemical exchange of water molecules in the hydration sphere of the Mn^{++} ion. However, their suggestions appear to overlook the fact that the correlation time for a direct dipole interaction has to be the tumbling time of the molecule.

Since, in general, to have a difference between $\underline{T}_1$ and $\underline{T}_2$ there must be a randomly fluctuating perturbation with a long correlation time, Bloembergen (15) suggests that the perturbation is an isotropic $A\,\underline{I}\cdot\underline{S}$ interaction between the spins $\underline{S}$ of Mn^{++} and the nuclear spins $\underline{I}$ of the protons in the first hydration shell, i.e., in $Mn(H_20)_6^{++}$. This type of hyperfine interaction which was used by Solomon and Bloembergen (16) to explain the measured relaxation times of hydrogen and fluorine in anhydrous hydrofluoric acid, leads to a set of equations similar to the ones derived for the dipole-dipole interaction. These equations which are obtained from a straightforward application of equation A9 of Solomon and Bloembergen (16) and equation 13 of Solomon (12) are

$$\left(\frac{1}{\underline{T}_1}\right)_{hf} = \frac{2}{3} S(S+1)(A/\hbar)^2 \, \underline{p} \left[\frac{\tau_S}{1+(\omega_{\underline{I}} - \omega_{\underline{S}})^2 \tau_S^2}\right] \qquad (13)$$

$$\left(\frac{1}{\underline{T}_2}\right)_{hf} = \frac{1}{3} S(S+1)(A/\hbar)^2 \underline{p}\left[\underline{\tau}_S + \frac{\underline{\tau}_S}{1+(\underline{\omega}_I - \underline{\omega}_S)^2 \underline{\tau}_S^2}\right] \qquad (14)$$

where $\underline{p}$ is the fraction of water protons coordinated to a manganese ion. In the transcription of the formulae of references 12 and 16, A^2 has been replaced by $A^2S(S+1)/3/4$ since the original formulae were derived for the case of $S = \frac{1}{2}$. The $A\underline{I}\cdot\underline{S}$ interaction contributes significantly to the relaxation times in Mn^{++} solutions because of the long relaxation time $\underline{\tau}_S$ of the Mn^{++} electrons. For Mn^{++} solutions $\underline{\tau}_S$ is about 3×10^{-9} sec which is larger than that of most other hydrated paramagnetic ions. As can be seen from a comparison of equations 11 and 13, the contribution of $(1/\underline{T}_1)_{hf}$ at high frequencies, is small compared to $(1/\underline{T}_1)_{dp}$ because of the large value of the denominator term $1 + (\underline{\omega}_I - \underline{\omega}_S)^2 \underline{\tau}_S^2$. However, at these frequencies $(1/\underline{T}_2)_{hf} > (1/\underline{T}_2)_{dp}$.

The $\underline{\tau}$ which appears in equations 13 and 14 should really be either the paramagnetic relaxation time or the chemical exchange time for the protons of the first hydration shell, whichever is shorter. The fact that the $\underline{T}_1/\underline{T}_2$ anomaly occurs to a large extent only for Mn^{++} solutions supports the use of the paramagnetic relaxation time.

As pointed out by Bloembergen, a contribution to $1/\underline{T}_1$ is expected according to equation 13 when $\underline{\omega}_S\underline{\tau}_S = 1$. The dispersion shown in figure 1, of $1/\underline{T}_1$ at a proton angular frequency $(\underline{\omega}_I)$ of ca. 4×10^5 radius sec^{-1} corresponds to a $\underline{\omega}_S$ of 2.5×10^8 radius sec^{-1} for the electron, so that indeed $\underline{\omega}_S\,\underline{\tau}_S = 1$ at this point. Equations 13 and 14 further correctly predict that at low frequencies, $\underline{T}_1 = \underline{T}_2$. However, the theory is incomplete since it does not explain the second

region of dispersion of $1/T_1$ starting at 10 Mc (proton frequency).

One requirement for the occurrence of the anomaly, independent of whether the dipole-dipole interaction or the hyperfine interaction is used, is the existence of water molecules in the coordination shell of Mn^{++}. The explanation using the hyperfine interaction also requires the existence of a long paramagnetic relaxation time.

We have endeavored to test these ideas by performing experiments in which the coordinated water molecules have been partially or wholly displaced from the Mn^{++} hydration sphere by chelating agents. In complexing the Mn^{++}, the electron relaxation time τ_S is also shortened.

Experimental

1. Chemicals

The uncomplexed manganese experiments, $Mn(H_2O)_6^{++}$ were done with reagent grade $MnCl_2 \cdot 4\ H_2O$ as the manganese source. It was weighed as such.

The chelating agents used were ethylenediaminetetraacetic acid (H_4Y) and nitrilotriacetic acid (H_3X). The former is a hexadentate chelating agent which, in the complex, occupies all six of the positions in the coordination sphere of the manganese ion. Its structure is represented by the formula

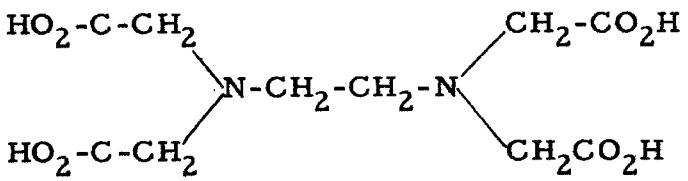

The MnY^{-2} solutions were prepared from reagent grade $Na_2H_2Y \cdot 2\ H_2O$ and reagent grade manganous chloride. The solutions

were prepared by adding $\underline{x}$ moles of Mn^{++} to a solution containing $\underline{y}$ moles of H_2Y^{-2} and $(\underline{y}+\underline{z})$ moles of NaOH; the resulting solutions contained $\underline{x}$ moles of MnY^{-2}, $\underline{z}$ moles of HY^{-3} and (y-x-z) moles of H_2Y^{-2}. A typical stock solution contained 0.125 $\underline{M}$ MnY^{-2}, 0.05 $\underline{M}$ H_2Y^{-2}, 0.075 $\underline{M}$ HY^{-3}, at a pH of ca. 6.3.

The equilibria used to calculate the molar concentrations are (17)

$$H_2Y^{-2} \rightleftharpoons HY^{-3} + H^+ \quad K_3 = 6.9 \times 10^{-7}$$

$$HY^{-3} \rightleftharpoons Y^{-4} + H^+ \quad K_4 = 5.49 \times 10^{-11} \qquad (15)$$

$$Mn^{++} + Y^{-4} \rightleftharpoons MnY^{-2} \quad K_f = 3.17 \times 10^{13}$$

The nitrilotriacetic acid (H_3X), whose structural formula is

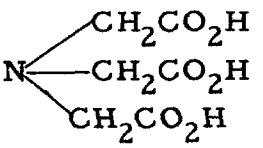

can occupy four positions in the coordination sphere of the manganese in the 1:1 complex, MnX^{-1}, or all six positions in the 1:2 complex, MnX_2^{-4}. In order to obtain the equilibrium data necessary for the analysis of the Mn^{++} - H_3X system, pH titrations, using standard NaOH, were done on a solution containing the free acid (H_3X), and solutions of the acid containing 40% Mn^{++}, and 90% Mn^{++}. The resulting curves are shown in figure 2. Since H_3X is only sparingly soluble in water the break in curve I due to the titration of the first proton was not observed.

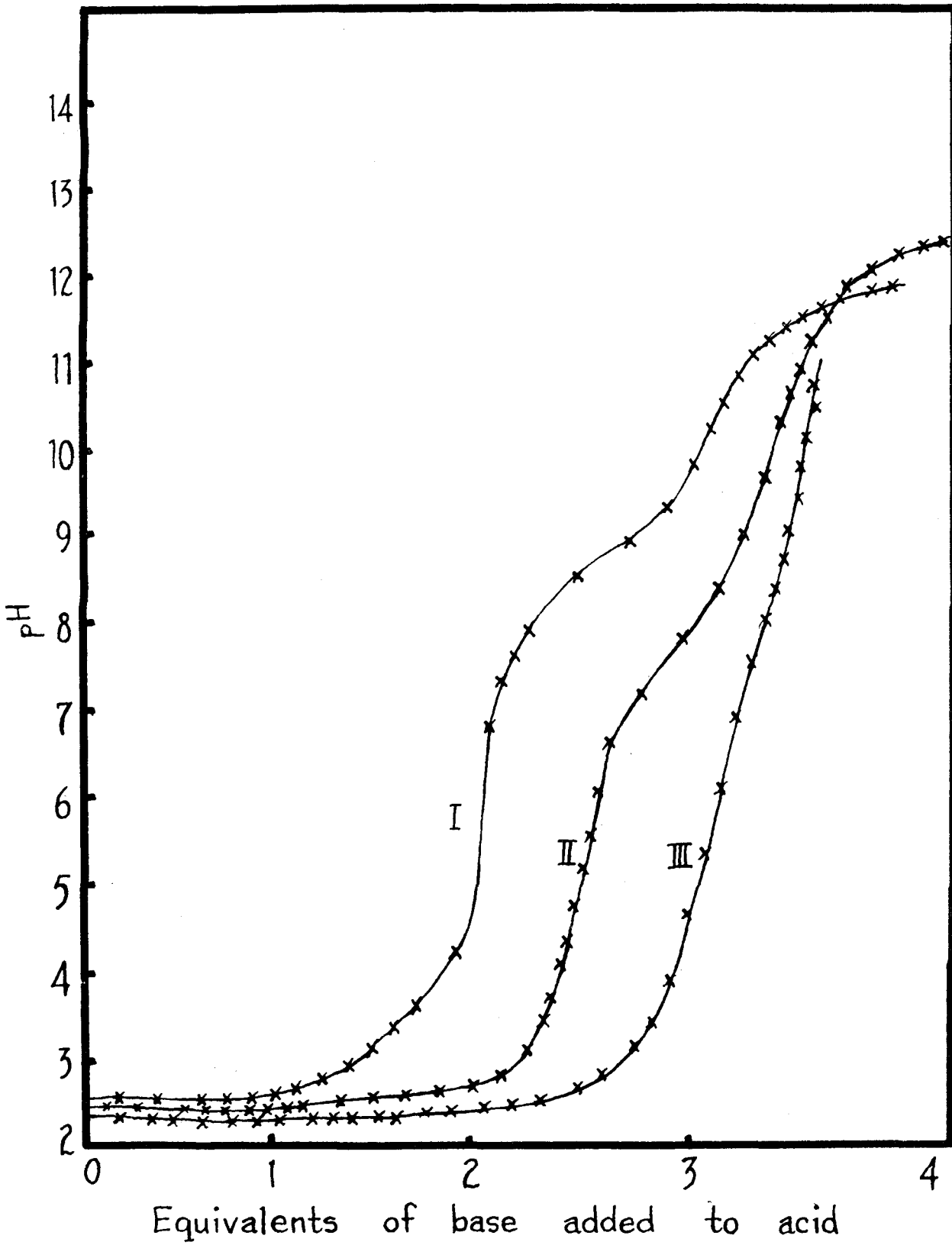

Fig. 2

Titration Curves for Mn^{++}-Nitrilotriacetate System

During the titration it was found that the ratio of the equivalents of base added to the equivalents of acid present had to be 1.5 before the acid was completely dissolved. The break due to the titration of the second proton is clearly seen. From curve I we were able to obtain the values 3.05 and 9.25 for pK_2 and pK_3, respectively. Martell and Calvin (17) give the following values for the above quantities.

$$pK_2 = 3.07 \text{ at ionic strength of zero}$$
$$= 2.49 \text{ at ionic strength of } 0.1$$
$$pK_3 = 10.70 \text{ at ionic strength of zero}$$
$$= 9.73 \text{ at ionic strength } 0.1$$

The two breaks in curve II correspond to the 1:1 and 1:2 Mn^{++} - H_3X complexes. Two breaks are not shown by curve III since the formation of MnO_2 at high pH's necessitated the termination of the titration. From the difference between the first equivalence points of the three curves, the concentration of Mn^{++} in the solutions could be determined. This value was used in calculating the molar concentrations of the Mn^{++} X^{-3} complexes. The equilibrium constants obtained from the curves are

$$Mn^{++} + X^{-3} \quad MnX^{-1} \qquad K_{1f} = 10^7 \underline{M}^{-1}$$
$$MnX^{-1} + X^{-3} \quad MnX_2^{-4} \qquad K_{2f} = 5 \times 10^3 \underline{M}^{-1} \qquad (16)$$

Solutions were prepared by adding $\underline{a}$ moles of Mn^{++} to a solution containing $\underline{b}$ moles of HX^{-2} and $\underline{b}$ moles of X^{-3}, obtained by titrating a solution initially containing solid H_3X to a pH of 9.25 with standard sodium hydroxide. The resulting solutions contained $(\underline{b}-\underline{a})$ moles of MnX_2^{-4}, $(2a-b)$ moles of MnX^{-1}, and $\underline{b}$ moles of HX^{-2}.

(In the most dilute solution, allowance was made for the dissociation of MnX_2^{-4}.) In all such solutions, $(Mn^{++})/(MnX^{-1}) < 0.01$.

2. Relaxation Time Measurements:

The relaxation times were measured using a Varian Associates V-4300 High Resolution NMR Spectrometer with a 12" magnet operating at 40 Mc. This instrument operates on the principle of Nuclear Induction, first introduced by Bloch (8). In this method the change of the magnetization in the system at resonance is detected and displayed on an oscilloscope or graphic recorder in the form of an absorption or dispersion curve.

If the x, y, and z components of the vector product $\gamma \underline{M} \times \underline{H}$ in equation 7 are added to equations 9 and 10, the following equations which express the total change of $\underline{M}$ with time are obtained:

$$\begin{aligned} \dot{M}_x &= \gamma (M_y H_o + M_z H_1 \sin \omega t) - M_x/\underline{T}_2 \\ \dot{M}_y &= \gamma (M_z H_1 \cos \omega t - M_x H_o) - M_y/\underline{T}_2 \\ \dot{M}_z &= -\gamma (M_x H_1 \sin \omega t + M_y H_1 \cos \omega t) + (M_o - M_z)/\underline{T}_1 \end{aligned} \tag{17}$$

The method used to measure $\underline{T}_1$ is based on the solution of these equations for the case which Bloch calls "rapid passage". The necessary conditions for this are that the instrument be tuned for a dispersion signal, and that $1/\gamma H_1 <<$ time at resonance $<< \underline{T}_2$ and $\underline{T}_1$. The solution of equations 17 for the case of "rapid passage" is (1)

$$M(t) = \int_{-\infty}^{t} \frac{dt' M_o(t) \delta(t')}{\underline{T}_1 (1+\delta^2(t'))^{\frac{1}{2}}} \exp\left[\int_{t}^{t'} \frac{\delta^2(t'') + \underline{T}_1/\underline{T}_2 \, dt''}{\underline{T}_1 (1+\delta^2(t''))}\right] \tag{18}$$

where the quantity $\underline{\delta}$ is a measure of the distance off resonance. It is defined by

$$\underline{\delta} = (\underline{\omega}_o - \underline{\omega}) / \gamma \underline{H}_1$$

where $\underline{\omega}_o$ is the Larmor frequency at resonance. If $\delta^2 >> T_1/T_2 \geq 1$ and M_0 assumed to be constant, equation 18 becomes

$$M(t) = \frac{M_0}{\underline{T}_1} \int_{-\infty}^{t} dt' \exp \int_{t}^{t'} \frac{dt''}{\underline{T}_1} \tag{19}$$

In the actual experiments a sinusoidal modulating (H_o) sweep was used to pass through the resonance at a time t_o and return in a time t_r. If equation 19 is expressed in terms of these times one obtains

$$M(t) = \frac{M_0}{\underline{T}_1}\left[\int_{-\infty}^{t_o} \exp \frac{t'-t_o}{\underline{T}_1} dt' - \int_{t_o}^{t_r} \exp \frac{t'-t_o}{\underline{T}_1} dt' \right] \tag{20}$$

The last term is negative due to the change in sign of $\underline{\delta}$ in passing through resonance. Performing the integration, equation 20 becomes

$$M(t) = \frac{M_0}{\underline{T}_1} (2 - \exp \frac{t}{\underline{T}_1})$$

where $t = t_r - t_o$.

At the point where $\underline{M}(t) \longrightarrow 0$

$$\underline{T}_1 = t / \ell n\, 2 \tag{21}$$

The detailed method of measuring $\underline{T}_1$ was as follows. A sinusoidal modulating sweep of about 9 gauss at a frequency in the range of 0.1 to 0.5 cps was applied with the help of a Hewlett-Packard 202A Function Generator. In order to satisfy the condition $\delta^2 >> \underline{T}_1/\underline{T}_2$ the sweep was maintained entirely on the low field side of resonance

for a time of the order of $10\underline{T}_1$. The sweep was then rapidly expanded by manual adjustment of the oscilloscope X-amplitude knob so that there was a single sweep forward and back through resonance. The time spent at resonance could be controlled by increasing or decreasing the sweep range. Data were recorded on a Sanborn recorder which has a just barely sufficient high frequency response. By observing the times required above resonance to give a small upright signal and a small inverted signal, the time, t, above resonance for zero signal was determined.

In order to satisfy the conditions for rapid passage, the Varian instrument was used at its largest available H_1 ($\sim$0.075 gauss) which gives $1/\gamma H_1 = 0.0005$ sec. Time spent at resonance was about 0.02 - 0.05 sec. It was more difficult to satisfy the condition as regards $\underline{T}_2$ than $\underline{T}_1$. Because of the large value of H_1, it was usually not practicable to spin sample tubes containing conducting solutions, as there was too much leakage due to slight wobbling. By using 3 mm sample tubes instead of the standard 5 mm tubes, $\underline{T}_2$ values of 0.06 to 0.08 sec for non-spinning samples were obtained. The measured $\underline{T}_1$'s were in the range of 0.5 to 5 sec.

This method of measuring $\underline{T}_1$ gave the value 3.7 sec for pure degassed water which agrees with literature values (18). In order to decrease the proton-proton contribution and recognize the manganese-proton effect, $\underline{T}_1$ measurements were made in 50% by volume D_2O, for which $T_1 = 5.60$ sec in agreement with the value reported by Anderson and Arnold, 5.55, (19). Solutions were degassed with

bubbling nitrogen and tubes sealed off in a nitrogen atmosphere.

The method for measuring T_2 is based on the solution of equations 17 for the case of "slow passage". Using Bloch's nomenclature (20) we introduce the variables u and v, defined by

$$u = M_x \cos\omega t - M_y \sin\omega t$$
$$v = -(M_x \sin\omega t + M_y \cos\omega t) \tag{22}$$

With these, equations 17 become

$$\dot{u} + \frac{u}{T_2} + (\Delta\omega)v = 0$$
$$\dot{v} + \frac{v}{T_2} - (\Delta\omega)u = -\gamma H_1 M_z \tag{23}$$
$$\dot{M}_z + M_z/T_1 - \gamma H_1 v = M_o/T_1$$

where $\Delta\omega = \gamma H_o - \omega = \omega_o - \omega$

Under conditions of slow passage

$$\dot{u} = \dot{v} = \dot{M}_z = 0 \tag{24}$$

Solving equation 23 for v, we get

$$v = -\gamma H_1 M_z T_2 (1 + (\Delta\omega)^2 T_2^2)^{-1} \tag{25}$$

However,

$$M_z = M_o \frac{1 + (\Delta\omega)^2 T_2^2}{1 + (\Delta\omega)^2 T_2^2 + \gamma^2 H_1^2 T_1 T_2} \tag{26}$$

Then

$$v = \frac{-\gamma H_1 M_o T_2}{1 + (\Delta\omega)^2 T_2^2 + \gamma^2 H_1^2 T_1 T_2} \tag{27}$$

A plot of v vs $\Delta\omega$ leads to a Lorentzian shaped absorption curve whose amplitude is at a maximum when $\Delta\omega = 0$.

In measuring T_2, a small value of H_1 was used in order to avoid saturation. In the absence of saturation $\gamma^2 H_1^2 T_1 T_2 << 1$. Under these conditions equation 27 becomes

$$v = \frac{-\gamma H_1 M_o T_2}{1 + (\Delta\omega)^2 T_2^2} \tag{28}$$

At resonance $\Delta\omega = 0$ and

$$v_{max} = -\gamma H_1 M_o T_2 \tag{29}$$

At half maximum

$$v = v_{max}/2$$

and $$\Delta\omega = 1/T_2 \tag{30}$$

The line width at this point is equal to twice $\Delta\omega$. Then

$$T_2 = \frac{2}{\delta\omega} \tag{31}$$

where $\delta\omega$ is the line width measured in radius/sec.

Care was taken to obtain a symmetrical signal whose shape was essentially Lorentzian. Corrections for field inhomogeneity, since it also contributes to the line width, were made using pure water as a standard. These corrections were of the order of 2-3 cps.

The electron magnetic resonance spectra of uncomplexed manganese, $Mn(H_2O)_6^{++}$, and of the complexes MnX^{-1} and MnX_2^{-4} were obtained using a Varian V-4500 instrument with a 6" magnet operating in the X band (3.16 cm). This instrument, using a phrase-sensitive detector, produces the derivative of the absorption curve. From such a curve it is possible to calculate the relaxation time, $\underline{T}_2$, of the electrons in the system. In the systems studied it was assumed that $\underline{T}_1 = \underline{T}_2$ for the electrons.

Results

The NMR relaxation time measurements for the three systems studied are given in Tables I, II, and III. The T_1 relaxation times are corrected for the solvent using the relation

$$\left(\frac{1}{\underline{T}_1}\right)_{\text{total}} = \left(\frac{1}{\underline{T}_1}\right)_{\text{solvent}} + \left(\frac{1}{\underline{T}_1}\right)_{Mn^{++}} \qquad (32)$$

In the $\underline{T}_1$ measurements, the relaxation time for the solvent 50% H_2O-D_2O, was measured as 5.60 sec. The field inhomogeneity is given in the tables for $\underline{T}_2$ measurements by the width of the solvent line. The $\underline{NT}_2$'s given in the last column have been corrected for this effect.

The electron paramagnetic resonance spectra of Mn^{++}, MnX^{-1}, and mixtures thereof are exhibited in figure 3. The Mn^{++} spectrum shows the well-known fine structure (21), (22), due to the hyperfine interaction with the Mn^{55} nucleus. The spacing of the lines is about 92 gauss or 2.6×10^8 cps. The line width corresponds to T_2 (electrons) $= 3 \times 10^{-9}$ sec. The broad line observed for MnX^{-1} has a

TABLE I

Relaxation Time for Mn^{++} Solutions (aq. $MnCl_2$)

T_1 Measurements

Mn^{+2} M	t_d sec	t_r sec	t_a sec	T_1(total) sec	$T_1(Mn^{++})$ sec	$NT_1(Mn^{++})$ Msec
2.5×10^{-5}	40	0.075	2.03	2.93	6.10	1.53×10^{-4}
5×10^{-5}	30	0.050	1.30	2.02	3.15	1.57×10^{-4}
1×10^{-4}	25	0.050	0.79	1.15	1.44	1.45×10^{-4}

av. $1.57(\pm 0.05) \times 10^{-4}$

t_d = time spent down field before passing through resonance

t_r = time spent at resonance

t_a = time spent above resonance in order for the magnetization to go to zero.

T_2 Measurements

Mn^{++} M	$\delta\nu$ (total) cps	$\delta\nu$ (solvent) cps	$\delta\nu$ (Mn^{++}) cps	$T_2(Mn^{++})$ sec	NT_2 Msec
1×10^{-4}	3.15	1.22	1.93	0.165	1.65×10^{-5}
1×10^{-3}	19.90	1.30	18.60	0.017	1.70×10^{-5}
2×10^{-3}	42.20	1.90	40.30	0.0079	1.60×10^{-5}

Av. $1.65 (\pm 0.04) \times 10^{-5}$

$T_1/T_2 = 9.5 (\pm 0.05)$

TABLE II

Relaxation Times for Manganese-Ethylenediamine Tetraacetate (MnY^{-2}) System

MnY^{-2} M	t_d sec	t_r sec	t_a sec	Ti(total) sec	Ti(MnY^{-2}) sec	NTi Msec
6.0×10^{-5}	40	0.03	1.80	2.60	4.68	2.80×10^{-4}
1.05×10^{-4}	25	0.04	1.30	1.88	2.78	2.92×10^{-4}
3.00×10^{-4}	20	0.048	0.66	0.955	1.44	3.44×10^{-4}

av. $3.05\ (\pm 0.20) \times 10^{-4}$

T_2 Measurements

MnY^{-2} M	$\delta\nu$ (total) cps	$\delta\nu$ (solvent) cps	$\delta\nu$ (MnY^{-2}) cps	T_2(MnY^{-2}) sec	NT_2 Msec
1.50×10^{-2}	21.85	1.85	20.00	0.0159	2.39×10^{-4}
2.50×10^{-2}	30.60	1.85	28.75	0.0111	2.78×10^{-4}
3.13×10^{-2}	39.0	1.85	37.15	0.0086	2.69×10^{-4}

av. $2.62\ (\pm 0.15) \times 10^{-4}$

$T_1/T_2 = 1.5\ (\pm 0.12)$

TABLE III

Relaxation Times for Manganese-Nitrilotriacetate Solutions

$\underline{T}_1$ Measurements

MnX^{-1}	MnX_2^{-4}	t_r	t_a	T_1(total)	$T_1(Mn^{-2})$	$^*NT_1(MnX^{-1})$
$\underline{M}$	$\underline{M}$	sec	sec	sec	sec	$\underline{M}$sec
5.53×10^{-4}	1.78×10^{-4}	0.05	0.275	0.398	0.427	2.32×10^{-4}
2.71×10^{-4}	8.90×10^{-5}	0.05	0.55	0.795	0.916	2.48×10^{-4}
1.08×10^{-4}	2.56×10^{-5}	0.05	0.062	1.535	2.04	2.25×10^{-4}

av. $2.35(\pm0.09)\times10^{-4}$

*This value has been corrected for contributions by MnX_2^{-4} for which $\underline{NT}_2$ was measured as 7.4×10^{-4} $\underline{M}$ sec and $T_1 = T_2$.

$\underline{T}_2$ Measurements

MnX^{-1}	MnX_2^{-4}	$\delta\nu$(total)	$^*\delta\nu$(corr.)	$T_2(MnX^{-1})$	NT_2
$\underline{M}$	$\underline{M}$	cps	cps	sec	$\underline{M}$ sec
2.40×10^{-2}	2.38×10^{-2}	43.1	39.0	0.0082	1.96×10^{-4}
3.92×10^{-2}	5.4×10^{-3}	52.5	49.0	0.0065	2.54×10^{-4}
4.88×10^{-2}	6×10^{-4}	58.6	56.5	0.0056	2.75×10^{-4}

av. $2.42\ (\pm0.34)\times10^{-4}$

*This line width has been corrected for both MnX_2^{-4} and the solvent, H_2O.

$$\underline{T}_1/\underline{T}_2 = 1.04\ (\pm0.15)$$

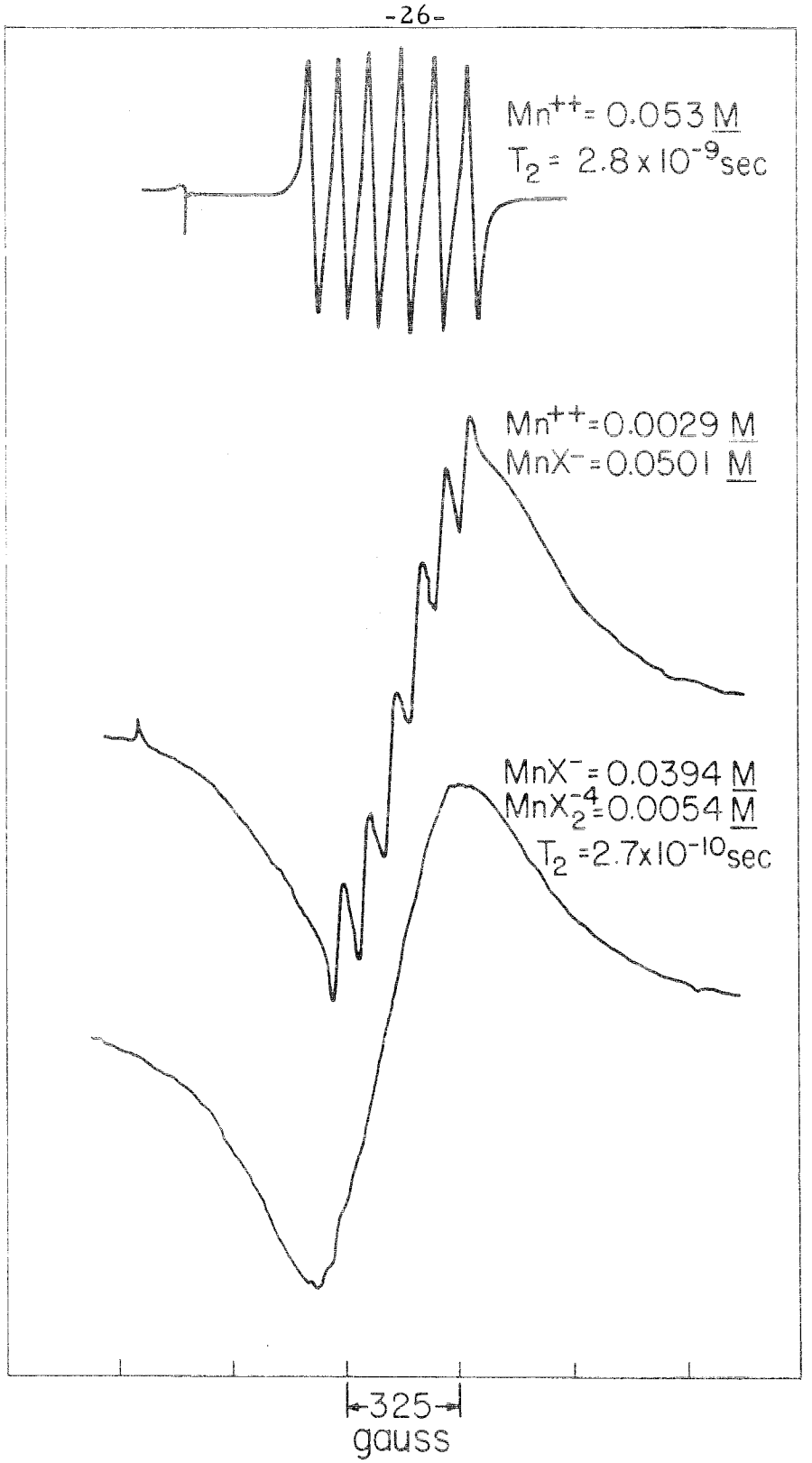

Fig. 3

EPR Spectra of Mn^{++} Solutions

half-width of 430 gauss, or $T_2 = 3 \times 10^{-10}$ sec. When both Mn^{++} and MnX^{-1} are present in the system, the spectrum has the form of the middle curve in figure 3. *In the discussion to follow, we assume that* $T_1 = T_2$ for the electrons.

Discussion

The results indicate that the abnormal $\underline{T}_1/\underline{T}_2$ ratio for protons in Mn^{++} solutions disappears when the manganese is complexed by suitable chelating agents. By such complexing, $\underline{T}_1$ is increased slightly due to the increased shielding of the Mn^{++} nucleus by surrounding ligands. A far larger increase is experienced by T_2. This large increase in $\underline{T}_2$ accounts for the fact that in Mn^{++} solutions containing chelating agents, the ratio T_1/T_2 decreases and approaches unity.

Both the dipole-dipole interaction and the isotropic hyperfine interaction can explain the increase of $\underline{T}_2$ in the manganese-ethylenediaminetetraacetic system. In the MnY^{-2} complex there are no water molecules in the first coordination layer of the manganese. In such a case any type of interaction which depends on the proximity of the water protons to the paramagnetic ion will be greatly diminished. Thus, the study of the proton relaxation time in the manganese-ethylenediaminetetraacetic acid system showed that the large value of $\underline{T}_1/\underline{T}_2$ for aqueous Mn^{++} solutions is due to some type of direct bonding between the proton and the manganese ion.

Presumably, there are still two water molecules attached to the manganese in the 1:1 complex between Mn^{++} and H_3X. The fact that $\underline{T}_1$ and $\underline{T}_2$ are equal in this system tends to rule out the possibility that the dipole-dipole interaction is the sole cause of the

$\underline{T}_1/\underline{T}_2$ anomaly. If this were the case one would expect $\underline{T}_1/\underline{T}_2$ for MnX^{-1} to be one third of that for Mn^{++}, or about 3.

From the study of the EPR spectra in the MnX^{-1} system, it appears that a long paramagnetic relaxation time is also required for the $\underline{T}_1/\underline{T}_2$ anomaly to occur. When Mn^{++} is complexed by nitrilotriacetate the electron relaxation time decreases by a factor of ten. This decrease is enough to cause the proton relaxation times to again be equal.

Using the value found in uncomplexed Mn^{++} solutions for the proton relaxation time, T_2, in equation 14, we find the value for (A/h) to be 1.21×10^6 cps. This value differs by a factor of ten from the one reported by Bloembergen (15), (2×10^5 cps.).

Conclusion

In conclusion, it should be pointed out that although the A $\underline{I} \cdot \underline{S}$ interaction explains part of the anomalous $\underline{T}_1/\underline{T}_2$ ratio of Mn^{++} solutions at 40 Mc, it cannot be the whole story. It is incomplete in that it does not explain the second region of dispersion of $1/\underline{T}_2$ at around 10 Mc. (proton frequency). It would be of interest to make studies in this frequency range similar to the ones above. Such an endeavor was not attempted in this investigation due to the unavailability of the variable-frequency equipment.

It should also be noted that the theory predicts an increase in $1/\underline{T}_2$ as well as in $1/\underline{T}_1$ when $(\omega - \omega_s)^2 \tau_s^2 = 1$ or when $\omega_s = 3.3 \times 10^8$ cps. However, the investigationsof Bloom (14) and Nolle and Morgan (13) indicate that $1/\underline{T}_2$ is independent of frequency up to 30 Mc. This point could also stand further investigation.

III. MAGNETIC RESONANCE STUDIES OF THE FERRIC FLUORIDE COMPLEXES

Electron Paramagnetic Resonance and Nuclear Resonance have also been found to be exceedingly useful in the study of complex formation in inorganic systems. The only requirement for such a study is for the species of interest to have an observable nuclear moment and/or electron moment. Solutions containing ferric ion (Fe^{+++}) and fluoride ion (F^-) satisfy both conditions.

The results of a preliminary investigation of the complexes found between ferric ion and fluoride ion in solution are reported in this section. A general discussion of the type of information one can obtain from such a study is also included.

Theory

In general, the nuclear resonance of the fluoride ion is relatively sharp and readily detected. The ion is very similar to the proton in its magnetic properties. As mentioned before, the proton gyromagnetic ratio is 2.66×10^4 radius sec^{-1} $gauss^{-1}$ while the ratio for fluoride ion is 2.55×10^4.

The technique of NMR has been used by Connick and Poulson (23) to study the complexes formed by fluoride and aluminum in solution. From such a study they were able to set a lower limit of 0.008 sec for the lifetime for exchange of fluoride between the species. Since Al^{+++} is diamagnetic, there was no apparent electron-nucleus interaction in the system.

Ferric ion (Fe^{+++}) and its isoelectric counterpart Mn^{++} are the most interesting of the first transition elements to study by EPR methods. These two ions are unique in that the 3d shell is now

half-filled and the free ion is thus in an $^6S_{5/2}$ ground state. This condition is optimum for the observation of paramagnetic resonance since there is no spin-orbit interaction which could cause the resonance phenomenon to be unobservable. If such an interaction were present it could split the electronic energy levels to such an extent that the externally applied radiation, used in EPR experiments, could not induce transitions between them.

Most of the EPR investigations of Fe^{+++} have been done on the alum salts. Unlike manganese, the abundant Fe^{+++} isotopes have zero nuclear spin and would not show any nuclear hyperfine structure. This limited the work on the ferric alums to a study of the effects of electron-lattice interactions (24), (25), (26), (27).

The complexing of Fe^{+++} by fluoride in acid solutions has been studied by Dodgen and Rollefson (28) at 25°, using a potentiometric method. Their work has since been extended to 15° and 35° by Connick and co-workers (29).

We have used the techniques of EPR and NMR to investigate the ferric fluoride complexes in both hydrofluoric acid and aqueous solutions of ammonium fluoride.

Experimental

1. Chemicals:

A ferric stock solution was prepared from C. P. ferric perchorate. The commercially available ferric perchlorate (G. F. Smith) was recrystallized three times from water. A known quantity of the salt was redissolved in puritas water to form the stock solution. The concentration of ferric ion in the solution was determined by the iodometric method given by Swift (30).

Reagent grade hydrofluoric acid was used in the HF experiments. The commercial hydrofluoric acid was assumed to contain 50% HF. The concentration of HF in the solutions used in the experiments was not critical since, in most cases, it was very much greater than the ferric ion concentrations. In the ammonium fluoride experiments, reagent grade NH_4F was used. It was weighed as such. Both the HF and NH_4F solutions were stored in polyethylene bottles. A known quantity of ferric ion was added to a solution containing fluoride just before the spectra were to be taken.

2. Measurements:

The electron resonance measurements were made with the Varian EPR spectrometer previously described. In these measurements, the samples were contained in small capillaries made from polyethylene tubing. During a run, the capillary containing the solution was located inside a 5 mm (o.d.) quartz tube which fitted snugly in the sample hole of the spectrometer.

It was possible to use the Varian Model 4300 B high resolution machine to study the F^{19} nuclear resonance in the NH_4F solutions. In these measurements the samples were contained in the standard 5 mm (o.d.) NMR tubes. If the machine was perfectly balanced for the highly conducting solutions, the sample tubes could be spun.

The high resolution machine could not be used for the HF solutions. Unsuccessful attempts were made to locate the F^{19} resonance in both concentrated and dilute solutions. The failure of the resonance to be observed is probably due to the peculiar fluoride relaxation times in the system. (Solomon and Bloembergen (16), in

investigating the relaxation times in HF solutions, found that the fluoride transverse relaxation time T_2 is considerably shorter than the longitudinal time T_1.) Therefore, the Varian wideline machine had to be used for these solutions. The samples were contained in 10 mm lucite plastic tubes which seem to be reasonably stable toward HF.

Results

1. Electron Resonance in NH_4F Solutions:

The EPR spectra of the ferric fluoride complexes showed some interesting results. When ferric ion is dissolved in a solution containing high concentrations of NH_4F, spectrum (a) in figure 4, is obtained. This spectrum consists of seven equally spaced lines of varying intensities. Such a spectrum is a definite indication of the existence of the $FeF_6^{\equiv\equiv}$ complex ion in the solution. The seven lines arise from the interaction of the six equivalent fluoride nuclei, each with spin 1/2, with the electron spins of the ferric ion. The interaction is of the form: $A\,\underline{I}\cdot\underline{S}$ where $\underline{I}$ is the sum of the nuclei spins of the fluorides and $\underline{S}$ denotes the electron spins. Such an interaction also explains the various intensities of the hyperfine lines. The width of the lines was measured as 10 ($\pm$1) gauss and the separation between them was found to be 25 gauss. The type of information which can be gained from such a spectrum will be described later.

L. Helmholtz and S. Weissman have also observed the $FeF_6^{\equiv\equiv}$ resonance in solution (31). Aside from this there are no other published experiments which definitely prove the existence of $FeF_6^{\equiv\equiv}$ in

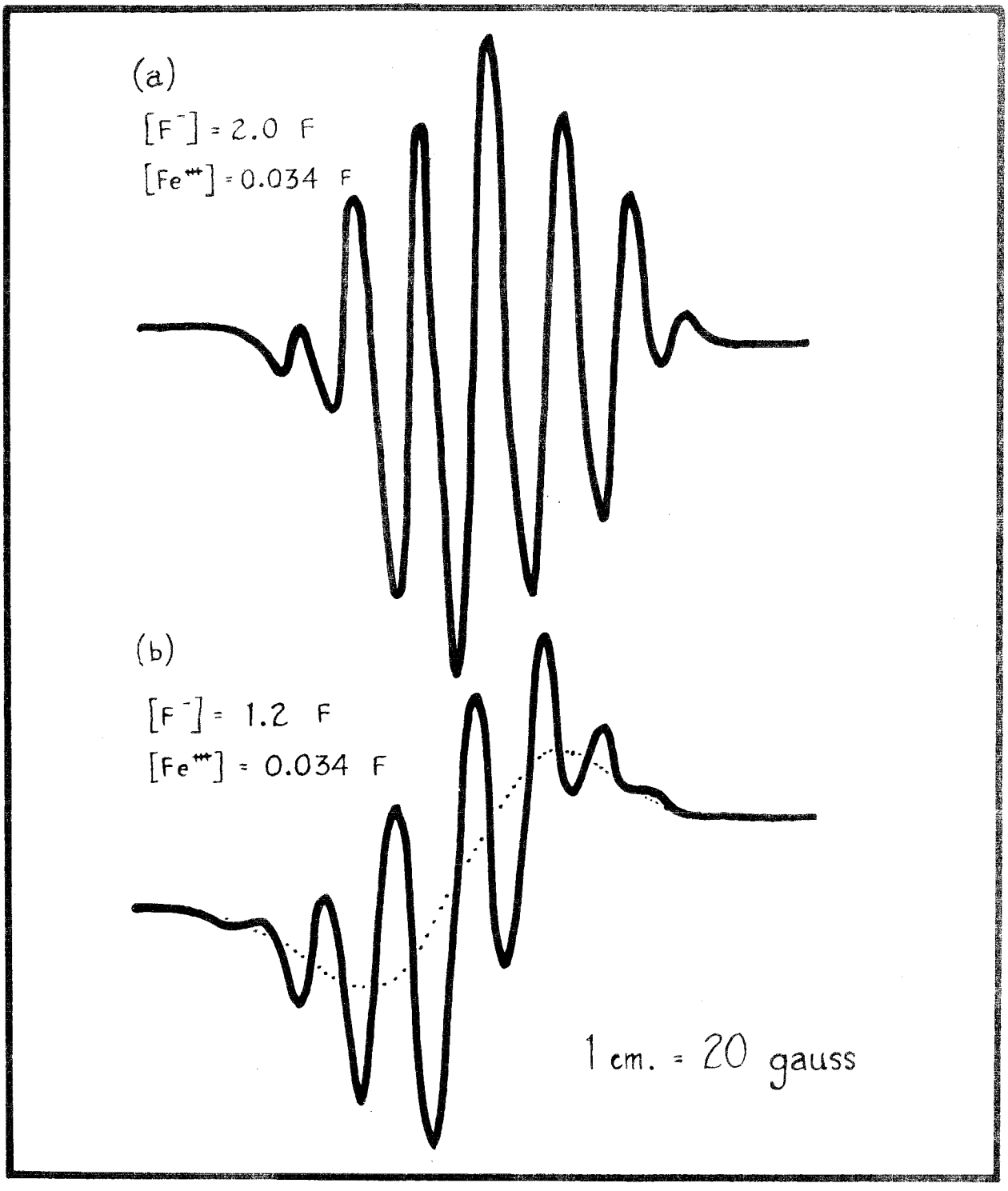

Fig. 4

EPR Spectra of $FeF_6^{\equiv}$ and $FeF_5^{=}$ in NH_4F Solutions

solution. Many salts of the type M_3FeF_6 are known where M can be either Na^+, Li^+, NH_4^+ or K^+.

If the fluoride concentration is decreased in the NH_4F solutions there appears a broader line superimposed on the hyperfine lines of the $FeF_6^{\equiv}$. This is spectrum (b) of figure 4. As the fluoride concentration is further decreased, the hyperfine lines disappear and one broad line remains. This line is found to broaden further with decreasing fluoride concentration. The width, ΔH, of the line changed from 58 to 644 gauss. These facts are shown by spectrums (a) and (b) of figure 5.

2. Electron Resonance in HF Solutions:

The EPR spectra of ferric ion dissolved in HF solutions were also obtained. These are shown by spectrums (c), (d), (e), and (f) of figure 5. Even the highly concentrated HF solutions did not show the characteristic hyperfine lines due to the presence of $FeF_6^{\equiv}$. We can conclude from this that $FeF_6^{\equiv}$ does not exist in any detectable amounts in hydrofluoric acid solutions. This conclusion agrees with that found by Low and Pryde (32), who showed that this complex did not exist in acid solutions by studying the potential of the ferrous-ferric half cell as a function of hydrogen fluoride concentration.

The width of the electron resonance line in the HF solutions was found to be constant at the value 180 gauss, as the HF concentration was decreased from 6F to 0.15 F. At this point the line broadened with decreasing HF concentrations, reaching the value 720 gauss in the solution containing equal moles of Fe^{+++} and F^-.

Spectrum (g) of figure 5 shows the EPR spectrum of a solution

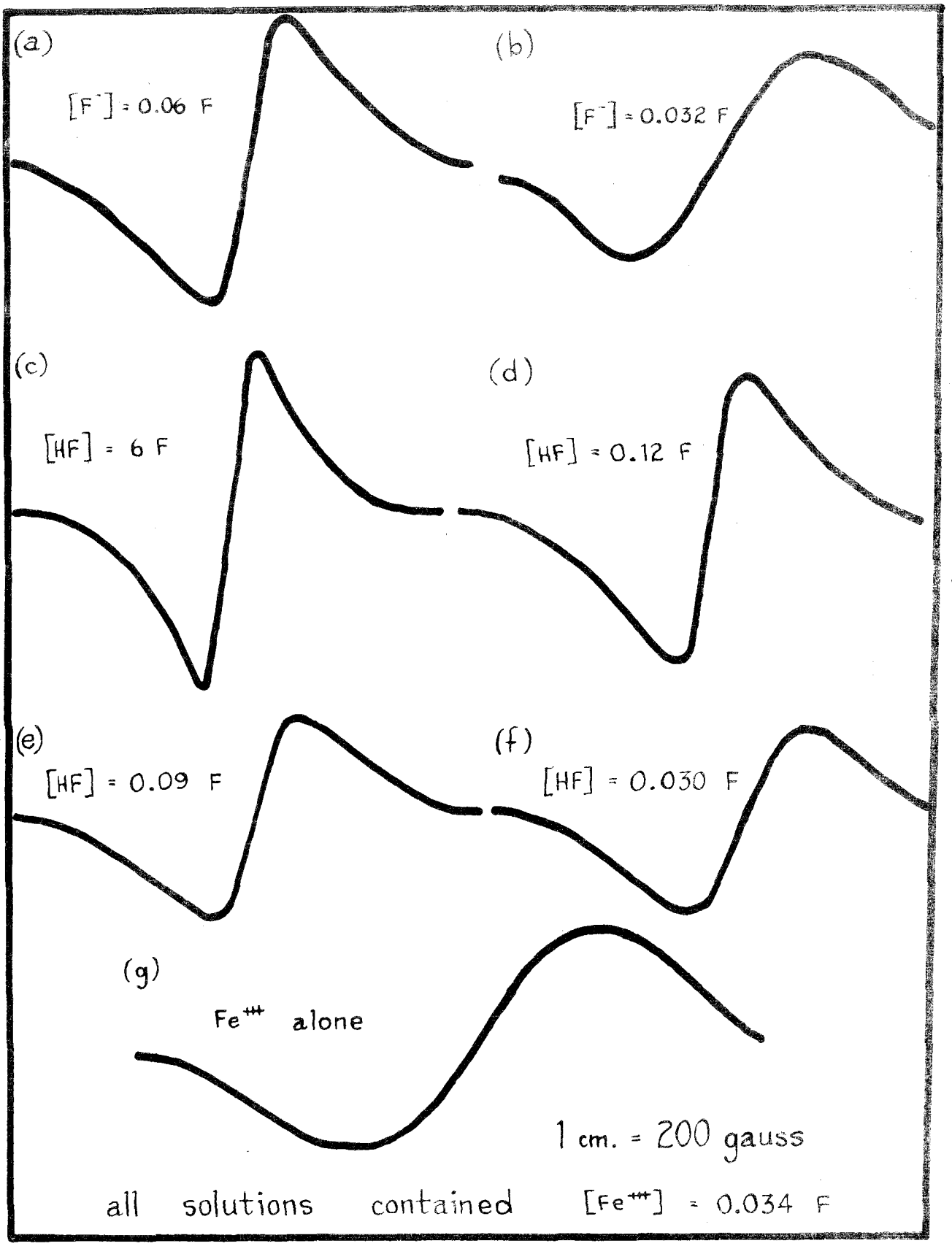

Fig. 5

EPR Spectra of the Lower Complexes

containing pure ferric perchlorate. In such a solution ferric ion exists primarily as the hexahydrate, $Fe(H_2O)_6^{+++}$. This is the first reported EPR spectra of the hydrated ferric ion in solution. The line width was measured to be 822 gauss which corresponds to an electron relaxation time of 1.35×10^{-10} sec. The formal concentrations are listed in the figures.

3. Nuclear Resonance in NH_4F Solutions:

The fluoride resonance line in concentrated ammonium fluoride solutions was found to be relatively sharp. In 8 M NH_4F the resonance line width was found to be 38 cps. There was not a perceptible change in the line width when 0.006 M ferric ion was added to the system. The above value represents the limit of solubility of ferric ion in 8 M NH_4F. Such a high concentration of fluoride ion was necessary in order to observe the resonance signal with the high resolution machine. Only a small shift of about 20 cps in the resonance line was observed between the pure NH_4F solution and the solution containing Fe^{+++}. This is just the shift expected from the change in the susceptibility of the system.

4. Nuclear Resonance in HF Solutions:

An unexpected phenomenon occurred in the HF solutions. As the ferric ion concentration was increased the amplitude of the fluoride resonance line decreased. There was no corresponding shift or broadening.

This behavior of the resonance signal could also be induced by heating the sample. The sample, contained in a lucite test tube,

was placed in a beaker of boiling water for approximately one minute. The tube was removed, dried, and immediately placed in the NMR apparatus. As the machine swept through resonance, no signal was recorded. Upon sweeping back and forth through resonance, the amplitude of the signal slowly increased until it reached its equilibrium value at room temperature (25^{o}). The temperature at which the signal first appeared was measured with a thermometer to be 40^{o}. Also, in this case, there was no apparent broadening or shift.

Discussion

1. The EPR Line Widths of the Ferric Fluoride Complexes

The increase in the EPR line widths in the HF solutions is found to be caused by the formation of the lower ferric fluoride complexes. We make the assumption, as did Dodgen and Rollefson (28), that only the complexes, FeF_3, FeF_2^+, and FeF^{+2} exist in the HF solutions. It shall be shown later that this is a valid assumption. We use the following equilibrium data, (28) (29), to calculate the molar concentrations of the species in the system.

$$\begin{aligned} Fe^{+3} + HF &\rightleftharpoons FeF^{+2} + H^+ && K_1 = 186 \\ FeF^{+2} + HF &\rightleftharpoons FeF_2^+ + H^+ && K_2 = 10.3 \\ FeF_2^+ + HF &\rightleftharpoons FeF_3 + H^+ && K_3 = 0.79 \end{aligned} \qquad (33)$$

The molar concentrations are given in Table IV along with the measured line widths. The formal concentration of Fe^{+3} is not listed, since it was constant at the value 0.034.

TABLE IV

EPR Line Widths of the Ferric Fluoride Complexes in HF Solutions

HF formula weight/ liter	Predominant complex	Molar conc. of complex	Line width in gauss
6	FeF_3	0.034	180 ($\pm$ 5)
0.30	FeF_3	0.028	180 ($\pm$ 7)
0.09	FeF_2^+	0.029	308 ($\pm$ 10)
0.03	FeF^{+2}	0.025	720 ($\pm$ 20)

The line width did not change in going from 6 formal HF to 0.30 formal. This is a very good indication that complexes higher than FeF_3 are not formed. It is highly unlikely that if FeF_4^-, for example, is present, its line width would be the same as FeF_3.

The fact that each complex gives rise to a characteristic line width is also shown from the study of the complexes in the ammonium fluoride solutions. We have already mentioned the seven hyperfine lines which are characteristic of the $FeF_6^{\equiv}$ complex. These lines have a half-width of 10 ($\pm$ 1) gauss. The broad line, which appears with the $FeF_6^{\equiv}$ lines when the NH_4F concentration is decreased, is undoubtedly due to the $FeF_5^{=}$ complex. It has a measured half-width of 57 ($\pm$ 1) gauss. The solution containing 0.034 formal Fe^{+3} and 0.064 formal F^- has a characteristic line width of 356 ($\pm$ 2) gauss which is just the value one would expect if the solution contained FeF_2^+ and a small amount of FeF^-. In the solution containing 0.034 formal Fe^{+3} and 0.032 formal fluoride, the primary species should be FeF^{++} and we would expect a line width close to 700 gauss. The actual width is 644 ($\pm$ 10) gauss which is a very good indication of the presence of the complex.

On the basis of the above data, we would expect the line width for the FeF_4^- complex to be intermediate between the values of 57 and 180 gauss. Since no such width was found even in 6 F HF we can safely conclude that this complex and higher complexes do not exist in any detectable amounts in HF solutions.

The electron relaxation time, being inversely proportional to the line width, is much shorter in solutions of the lower complexes. This decrease in T_2 of the electrons is probably due to the increased

asymmetry in the system. In going from $FeF_6^{\equiv\equiv}$ to $Fe(H_2O)_6^{+++}$, we substitute water molecules for fluoride ions in the hydration sphere of the ferric ion. From structural considerations one would expect the $FeF_6^{\equiv\equiv}$ complex to be quite symmetrical with a long electron relaxation time. However, the data also indicate that the complex with one water of hydration, $FeF_5(H_2O)^{=}$ has a shorter electron relaxation time than that containing five, $FeF(H_2O)_5^{++}$. From structural considerations one would not expect this to be the case. Perhaps, the difference in asymmetry in the two cases is due to some type of fast exchange reactions taking place which is dependent on the number of water molecules coordinated to Fe^{+3}. This could also account for the very short relaxation time for the $Fe(H_2O)_6^{+++}$ ion.

2. The Dissociation Constant for $FeF_6^{\equiv\equiv}$

We use the results obtained from the EPR study of the ferric fluoride complexes to calculate a value for the equilibrium constant of the reaction

$$FeF_6^{\equiv\equiv} \rightleftharpoons FeF_5^{=} + F^- \quad K_6 \tag{34}$$

The method is based on a comparison of the areas under the characteristic curves of $FeF_6^{\equiv\equiv}$ and $FeF_5^{=}$ from the spectrums in figure 4. Since the areas are directly proportional to the concentrations, we have only to determine their ratios to get a value for $\left[FeF_5^{=}\right] / \left[FeF_6^{\equiv\equiv}\right]$. If we assume Lorentzian line shapes, we find the ratio of the area of the $FeF_5^{=}$ line to that of the hyperfine

lines to be 1.14. Since the concentration of fluoride in the system is 1.2 formal, we calculate

$$K_6 = \frac{\left[FeF_5\right]\left[F^-\right]}{\left[FeF_6\right]} = (1.14)(1.01) = 1.15 \qquad (35)$$

where the molar concentration of fluoride ion has been used.

There have been no previous reported investigations of the equilibrium in equation 34. Babko and Kleiner (33), in studying the decolorization of the ferric thiocynate complexes by fluoride, obtained the value, 0.44, for the dissociation constant of $FeF_5^{=}$. Assuming their value to be correct, the value calculated for K_6 is not unreasonable, since one would expect $FeF_6^{\equiv}$ to be less stable than $FeF_5^{=}$.

The value for K_6 is at best only approximate, since the total fluoride concentration in the system was not known very accurately. Also, the width of the broad line due to $FeF_5^{=}$ could not be exactly determined since it was superimposed upon the fine structure lines of $FeF_6^{\equiv}$. Considering all of this, the EPR method still gave a reasonable value for the dissociation constant.

3. Shifts and Broadening of the Fluoride Resonance

The observed experimental results allow us to make a semi-quantitative discussion of the effects of dissolved ferric ions on the shifts and broadenings of the fluoride resonance in the solutions. With the value found for the coupling constant, A, we can calculate the relaxation time T_2, of the fluoride ions in the system. A knowledge of the coupling constant also allows us to make predictions as to the magnitude of the fluoride shifts one would expect from an

isotropic hyperfine interaction between the electrons of the ferric ion and the fluoride nuclei.

a. Nuclear Relaxation Times

The values of $\underline{T}_2$ for the complexed fluorides which arise from the interaction are given by equation 14,

$$\left(\frac{1}{T_2}\right)_{hf} = \frac{1}{3} S(S+1) (A/h)^2 \underline{p} \left[\underline{\tau}_S + \frac{\underline{\tau}_S}{1 + (\underline{\omega}_I - \underline{\omega}_S)^2 \underline{\tau}_2^2} \right] \qquad (14)$$

where $\underline{p}$ in this case is the ratio of the complexed to uncomplexed fluorides. Neglecting small second order effects, the value of the coupling constant, A/h, is given by the separation between adjacent peaks in the hyperfine spectrum of the $FeF_6^{\equiv}$ complex. This measured value is found to be 25 gauss or 7.0×10^7 cps. For ferric ion $S = \frac{5}{2}$ and the electron relaxation times, $\underline{\tau}_S$, are obtained from the EPR line widths. The nuclear relaxation times of the complexed fluorides in solutions containing high fluoride concentrations and the corresponding NMR line widths are given in Table V.

The line widths of approximately 10^6 - 10^8 cps are much too broad to be observed even with the wide line spectrometer. Therefore, only if there is rapid exchange between the fluorides in the system can one study the effects of the hyperfine interaction on the fluoride ions. The possibility of such an exchange taking place is discussed below.

TABLE V

NMR Relaxation Times of the Complexed Fluorides

Specie	τ_s sec	T_2 sec	$\delta\nu$ (cps)
$FeF_6^{\equiv}$	1.11×10^{-8}	1.6×10^{-9}	1.99×10^{8}
$FeF_5^{=}$	1.9×10^{-9}	9.26×10^{-9}	3.44×10^{7}
FeF_3	6.17×10^{-10}	2.86×10^{-8}	1.12×10^{7}
FeF_2^{+}	3.71×10^{-10}	4.75×10^{-8}	6.7×10^{6}
FeF^{++}	1.54×10^{-10}	1.14×10^{-7}	2.78×10^{6}

b. Shifts and Exchange Times in the Ferric Fluoride System

The shift, ΔH in cps, of the fluoride resonance in the ferric fluoride complexes due to the hyperfine interaction is related to the coupling constant, A, by

$$\Delta H = \frac{2\beta H_z \, S(S+1) \, A/h}{3RT} \tag{36}$$

where H_z is the applied magnetic field and the other symbols have their usual meanings. The magnetic field for the wide line NMR experiments was approximately 3×10^3 gauss. Under these conditions $2\beta H_z / 3kT = 4.5 \times 10^{-4}$. Using these values in equation 36 we find

$$\Delta H = 2.76 \times 10^5 \text{ cps} \tag{37}$$

If there is rapid exchange between the fluorides in the system, the observable average shift of the uncomplexed fluorides will be equal to

$$\Delta H_{av} = \Delta H \underline{p} \tag{38}$$

where, as before, p is the fraction of fluorides complexed. In order to see an effective shift in the uncomplexed fluoride resonance, the lifetime, t_f, of the fluoride in the uncomplexed state must be equal to or less than the reciprocal of the average shift in the system. Alternatively, since the lifetime, t_c, in the complexed state is

$$t_c = p t_f \tag{39}$$

the condition necessary for observation of the shift is

$$t_c < \frac{1}{\Delta H} \tag{40}$$

Since no shifts in the resonance lines were found in the solutions containing the ferric fluoride complexes, t_c must be greater than $1/\Delta H$ or

$$t_c > 3.62 \times 10^{-6} \text{ sec} \tag{41}$$

This condition requires that the exchange rate between complexed and uncomplexed fluorides be less than 2.76×10^5 sec.

4. The Fe^{+++}-F^- Bond in the $FeF_6^{\equiv}$ Complex.

As mentioned previously, the hyperfine structure in the $FeF_6^{\equiv}$ system arises from an AI·S interaction between the electron spins of the ferric ion and the nuclear spins of the fluoride. Jaccarino, Shulman and Stout (34) investigated the effects of such an interaction on the fluoride resonance in solid FeF_3. They found the fluoride resonance to be shifted approximately 120 gauss. As discussed below, the magnitude of this interaction also allows one to arrive at a semi-quantitative description of the nature of the orbitals occupied by the unpaired electrons in the $FeF_6^{\equiv}$ system, and to consider a very simple approximate model of the bonding in the complex.

The treatment described below was used by Shulman and Jaccarino (35) who studied the nuclear resonance behavior of the fluorides in solid MnF_2. In order to explain the observed resonance shifts in the system, they postulated a small degree of covalency in the F^- bond to the paramagnetic Mn^{++} ion. Using such a postulate they interpreted their results as indicating that

each Mn^{++}-F^- bond contained 0.48(±0.2%) 2s-character.

The fact that hyperfine structure was observed in the electron resonance of the $FeF_6^{\equiv}$ system required that the orbitals occupied by the unpaired electron have some fluorine s-character since only an electron in an s-orbital has a finite probability of being at the nucleus. In all likelihood this s-character arises from the 2s orbitals of the fluoride ion since these are available for bonding.

As pointed out by Shulman and Jaccarino (35), the coupling constant, A/h, produced by an electron in a pure 2s orbital in F^- is:

$$(A/h)_{2s} = (8/3)\pi g\beta\gamma_N\hbar \left|\Psi_{(o)}\right|^2_{2s} = 4.53 \times 10^{10} \text{ cps} \qquad (42)$$

where $\left|\Psi_{(o)}\right|^2_{2s}$ is the normalized probability of finding a 2s electron at the fluoride nucleus. We compare this value with the observed hyperfine coupling constant in the $FeF_6^{\equiv}$ complex to arrive at the percentage of 2s-character of the orbitals. Since there are five unpaired electrons in Fe^{+3} we write

$$2s \text{ character} = \frac{5(A/h)_{exp.}}{(A/h)_{2s}} = \frac{3.5\times10^8}{4.53\times10^{10}} = 7.72 \times 10^{-3} \qquad (43)$$

This value is actually the total amount of unpaired electron density at the fluoride nucleus which gives rise to the observed hyperfine splittings, and is probably the amount of 2s character possessed by the orbitals containing the unpaired electrons.

We can gain some insight into the nature of the bonding in the $FeF_6^{\equiv}$ system by considering a possible mechanism by which the unpaired electrons, initially in orbitals around the Fe^{+3} nucleus,

interact with the fluoride nucleus.

There exists both bonding and antibonding orbitals between the ferric ion and the fluoride ions. Since two electrons can be placed in each orbital, there is room for four electrons between each fluoride and the Fe^{+3} ion. However, only three electrons are present, namely, two from the F^- ion and one 3d electron from the Fe^{+3} ion. If we use two of these electrons to form a covalent bond between the species, we are left with one electron in the antibonding orbital. This unpaired electron can interact with the fluoride nucleus, giving use to the observed hyperfine splittings.

The above treatment is probably highly oversimplified. However, it does suggest that there is some covalency in the $Fe\text{-}F^-$ bond. The exact magnitude of the covalency is in all likelihood very difficult to ascertain and will not be attempted here.

Conclusion

The above discussion shows the many facts which can be acquired from a study of inorganic complexes, using the techniques of EPR and NMR. The reported study of the ferric fluoride complexes is by no means complete. One fact which is still unexplained is the peculiar behavior of the nuclear resonance signals in the HF solutions. Future investigations of the system will probably solve the mystery.

IV. SUSCEPTIBILITY SHIFTS IN PARAMAGNETIC SOLUTIONS

The role of the magnetic susceptibility in producing nuclear resonance shifts was first investigated by Dickinson (36). Since the shifts in the resonance line are due to the fact that the nuclei experience different magnetic fields, he considered the field acting at a nucleus due to the present of paramagnetic ions in the solution. This field which he called H', is made up of three components.

$$H' = \underline{H}_1 + \underline{H}_2 + \underline{H}_3 \qquad (35)$$

The field $\underline{H}_1$, which is not to be confused with the radiofrequency applied field, arises from the magnetization produced by the paramagnetic ions outside a hypothetical spherical cavity which contains the nucleus. This is the well-known Lorentz cavity field and has the value $(4\pi/3)\,\underline{M}$, where $\underline{M}$ is the total magnetization in the solution. The component, $\underline{H}_2$, is the demagnetizing field. It is the field at the nucleus which opposes the large externally applied field, H_o. Its value is dependent on the shape of the vessel containing the solution. For the type of cylindrical tubes used in NMR experiments, it has the value, $-2\pi\underline{M}$. The fields $\underline{H}_1$ and $\underline{H}_2$ produce what is commonly called the isotropic susceptibility shift in the system.

The field, $\underline{H}_3$, is due to the paramagnetic ions inside the hypothetical sphere. If these interact with the nucleus through a dipole-dipole coupling, their effect should average to zero due to the random tumbling of the species.

However, Dickinson found experimentally that $\underline{H}_3$ was not in general equal to zero. Accordingly, he defined an interaction factor, $\underline{q}$, which is the ratio of the field, $\underline{H}_3$, to the total magnetization, $\underline{M}$, in the system. In order to explain the observed shifts, he had to assume that the quantity, $\underline{q}$, could be either positive or negative.

If the values for $\underline{H}_1$, $\underline{H}_2$, and $\underline{H}_3$ are substituted in equation 35, one sees that the field acting at the nucleus is directly proportional to the susceptibility in the system

$$H' = \frac{4\pi}{3}\,\underline{M} - 2\pi\underline{M} + q\underline{M} = -\left(\frac{2}{3}\pi - q\right)\underline{M} \qquad (36)$$

or, since $\underline{M} = \chi H_o$, where χ is the magnetic susceptibility

$$H' = -\left(\frac{2\pi}{3} - q\right)\chi H_o \qquad (37)$$

In measuring shifts in paramagnetic solutions, the pure solvent is usually used as the reference standard. In this case, the shift is equal to

$$\Delta H = \left(\frac{2\pi}{3} - q\right)\left(\chi - \chi_{solvent}\right) H_o \cong \left(\frac{2\pi}{3} - q\right)\chi H_o \qquad (38)$$

since the magnetic susceptibility of the paramagnetic solution is much greater than that of the solvent. If q were zero, the resonance line would be shifted to higher fields, since χ for a paramagnetic solution is positive. A positive value of q would tend to decrease the shift, while a negative value would enhance it.

Bloembergen (37) suggested that the non-zero values of q, found by Dickinson, arise from the anisotropy of the complex formed between the ion containing the nucleus and the paramagnetic ion in the solution. He derived the following expression for $\underline{q}$ in terms of

the anisotropic g-factor of the complex.

$$q = (16\pi b^3/45a^3)(g_{\parallel}^2 - g_{\perp}^2)/g^2 \qquad (39)$$

where $g_{\parallel}$ and $g_{\perp}$ are effective g-values depending on whether the instantaneous angle between the axis of the internal electric field, acting at the complex, and the magnetic field $\underline{H}_o$ is zero or ninety degrees. The quantity $\underline{b}$ is the assumed radius of the hypothetical sphere enclosing the complex and $\underline{a}$ is the distance between the two ions in the ion pair. This theory accounts for both positive and negative values of $\underline{q}$, depending on the relative magnitudes of $g_{\parallel}$ and $g_{\perp}$.

In a number of the solutions examined by Dickinson, it is possible that the type of $\underline{A}\underline{I}\cdot\underline{S}$ interaction, used previously to explain the resonance behavior in manganese and ferric fluoride solutions, also contributes to the non-zero values of q.

We have endeavored to differentiate between the two effects by measuring the paramagnetic susceptibility shifts in both organic and inorganic solutions.

Experimental

Since the shifts in the system are of relatively small magnitudes ($\sim$ 50 cycles), a method based on the use of an external standard was employed. A cell, similar to the one proposed by Reilly, McConnell and Meisenheimer (38) and by Zimmerman and Foster (39) was used. A cross section of the cell is shown in figure 6. It consists of two cylindrical coaxial glass tubes. The pure solvent is placed in

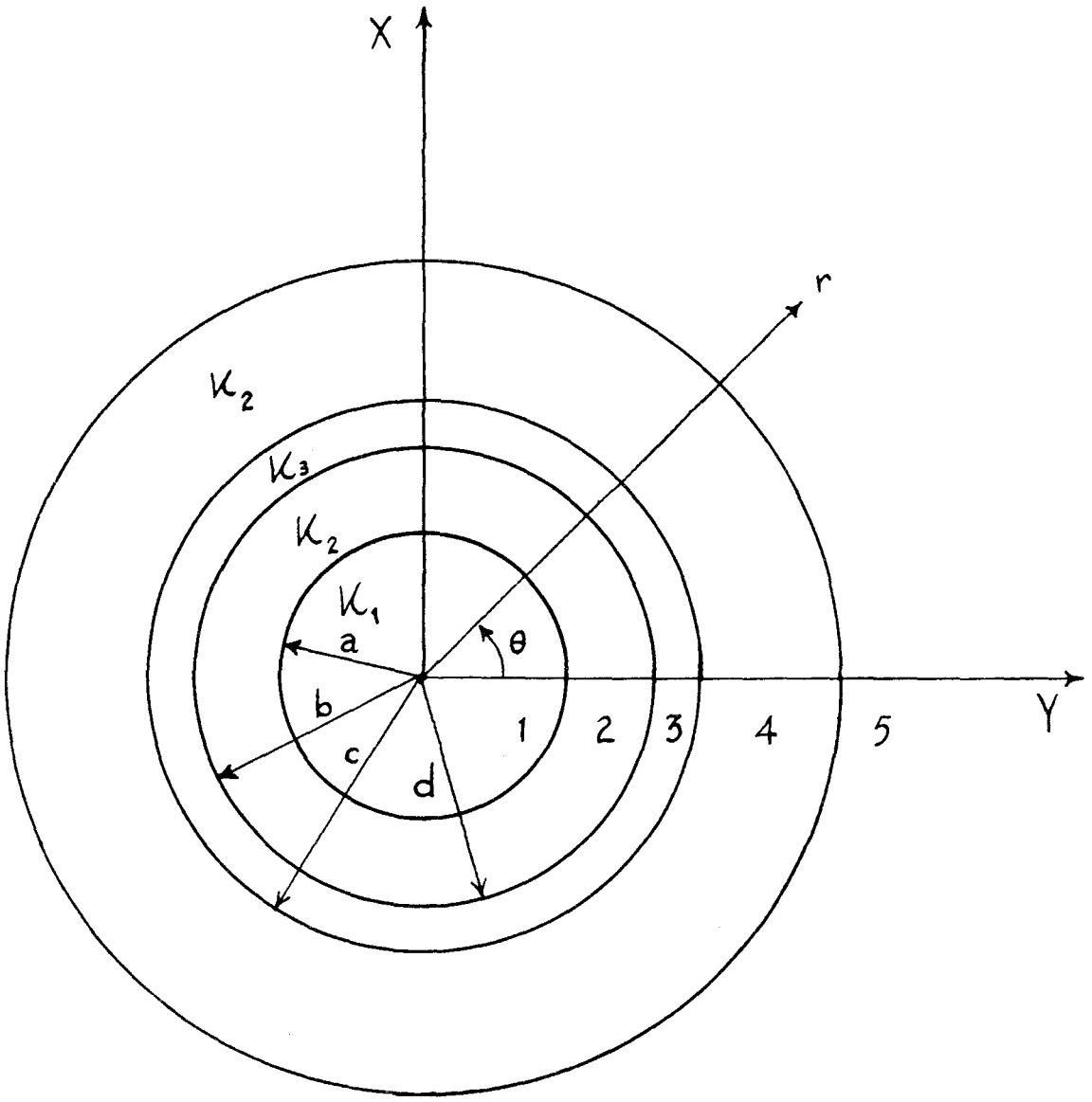

Fig. 6
Cross Section of Annular Cell

the annular region between the outer diameter of the inner tube and the inner diameter of the outer tube, while the paramagnetic solution is contained in the core or inner tube. In the figure the applied magnetic field is along the z axis. The following symbols are used.

$2a$ = internal diameter of inner tube

$2b$ = external diameter of inner tube

$2c$ = internal diameter of outer tube

$2d$ = external diameter of outer tube

χ_1 = magnetic susceptibility of liquid in center tube

χ_2 = magnetic susceptibility of glass

χ_3 = magnetic susceptibility of liquid in annulus

r = radius vector

θ = angle between radius vector and z axis

(1) = region of space for which $0 \leqslant r \leqslant a$

(2) = region of space for which $a \leqslant r \leqslant b$

(3) = region of space for which $b \leqslant r \leqslant c$

(4) = region of space for which $c \leqslant r \leqslant d$

(5) = region of space for which $d \leqslant r$

In using such a cell one must be certain that the field in the core is not dependent on the type of material in the annulus and vice-versa. The calculation presented in the Appendix shows that this condition is satisfied if the system is rotated. In this case

$$\langle H_1 \rangle = \text{average field in region (1)} = H_o \left[1 - \frac{2\pi}{3} \chi_{o_1} \right] \tag{45}$$

and

$$\langle H_3 \rangle = H_o \left[1 - \frac{2\pi \chi_{o3}}{3} \right] \tag{46}$$

Thus we see that the fields are only dependent on the applied magnetic field, $\underline{H}_o$, and the susceptibilities in the respective regions.

Measurement of Shifts

All spectra were taken at 25° with the high resolution NMR spectrometer.

Shifts of the proton resonance in benzene and in acetone, due to the paramagnetic organic free radical, 2-2 diphenyl -2- picryl hydrazyl (DPPH), were measured in order to study the susceptibility effects in an electrically neutral solution.

In order to prepare the radical, the corresponding hydrazine had first to be prepared. This was done by treating 37.575 grams of the commercially available diphenyl hydrazine hydrogen chloride with aqueous sodium hydroxide in order to remove the HCl. The mixture was filtered and while the diphenyl hydrazine was still on the filter paper, it was treated with just enough hot chloroform to dissolve it. To this solution was added a solution containing 24.20 grams of picryl chloride in chloroform. The mixture was heated strongly until a red-brown color appeared and a small amount of diphenyl hydrazine hydrogen chloride separated out. The solution was allowed to stand for about an hour. The diphenyl hydrazine hydrogen chloride was filtered off and the filtrate evaporated down to 15 ml. Approximately 30 ml of absolute ethyl alcohol were then added. Upon cooling very slowly, 3 grams of the diphenyl picryl hydrazine separated out. The product was recrystallized from glacial acetic acid.

To prepare the radical, six grams of the hydrazine were dissolved in 90 ml of dry pure chloroform (the chloroform was dried over anhydrous

sodium sulfate). Seventy grams of lead dioxide and five grams of anhydrous sodium sulfate were added. The solution was allowed to stand for one hour. It was then shaken and the deep violet solution filtered to remove the lead slime. The greater part of the chloroform was distilled off in a vacuum and the residue was treated with twice its volume of anhydrous ether. After several hours, violet-black, prism-like crystals approximately $\frac{1}{2}$ cm long appeared in the solution. These were filtered off and washed with alcohol. The permanganate-like crystals were purified by dissolving them in a small amount of hot chloroform, and treating the mixture with diethyl ether. After the solution had been allowed to stand for one hour, the radical was obtained in a very pure form.

The DPPH was found to be more soluble in acetone than in benzene. Saturated solutions in both solvents were prepared. Using the calibration curve of Poirier, Kahler, and Benington (40), the concentration of the DPPH was determined by dissolving 0.1 ml of the saturated solution in 49.9 ml of chloroform and measuring the optical density at 530 mu.

The measured shifts, along with the theoretical shifts calculated from equation 38, assuming q = 0, are shown in Table VI. The susceptibility of the DPPH solution was calculated using Curie's law.

$$\chi_0 = (N/V)\,\frac{\mu^2}{3kT} \qquad (40)$$

where N/V is the number of moles per unit volume and μ is the effective magnetic moment of the free radical, which was taken to

TABLE VI

SHIFTS OF SOLVENT PROTON DUE TO DPPH

(DPPH) M	Solvent	ΔH (theory) (Milligauss)	ΔH (experimental) (Milligauss)
0.0634	benzene	1.671	1.61 (±0.02)
0.1655	acetone	4.36	4.33 (±0.07)

be that due to a single electron. It has the value 0.92732×10^{-20} erg grams^{-1}.

The influence of a positive paramagnetic ion on the resonance of water protons and on the protons in the ammonium ion (NH_4^+) was studied using a solution containing hydrochloric acid, ammonium chloride, and cobaltous chloride ($CoCl_2$). As before, the susceptibility of the paramagnetic solution was calculated using Curie's law.

As first reported by Ogg (41), the spectrum of the NH_4^+ protons in strong acid consists of three lines due to the splitting of the proton energy levels by the N^{14} which has a nuclear spin, I = 1. This fact allowed the NH_4^+ protons to be easily distinguished from the protons in the H_2O molecules.

In figure 7, the shifts of both the ammonium and the water protons are plotted as a function of the cobaltous ion concentration. For comparison, the susceptibility shift, assuming q is zero, is also shown. The deviation of the water line from the theoretical curve can be explained if a q-value of 0.6 is assumed. The ammonium curve does not deviate very much from the theoretical one at low cobalt concentrations. However, at high concentrations, the shifts in the NH_4^+ protons are less than those predicted by the theory.

The greater shift of the ammonium protons as compared to those of water is clearly seen in figure 8. Initially, as seen from the top curve, the NH_4^+ protons appear down field from the H_2O. As the cobalt concentration is increased, the ammonium lines and the water lines appear at nearly the same field. At still higher concentrations the NH_4^+ resonance is at the higher field.

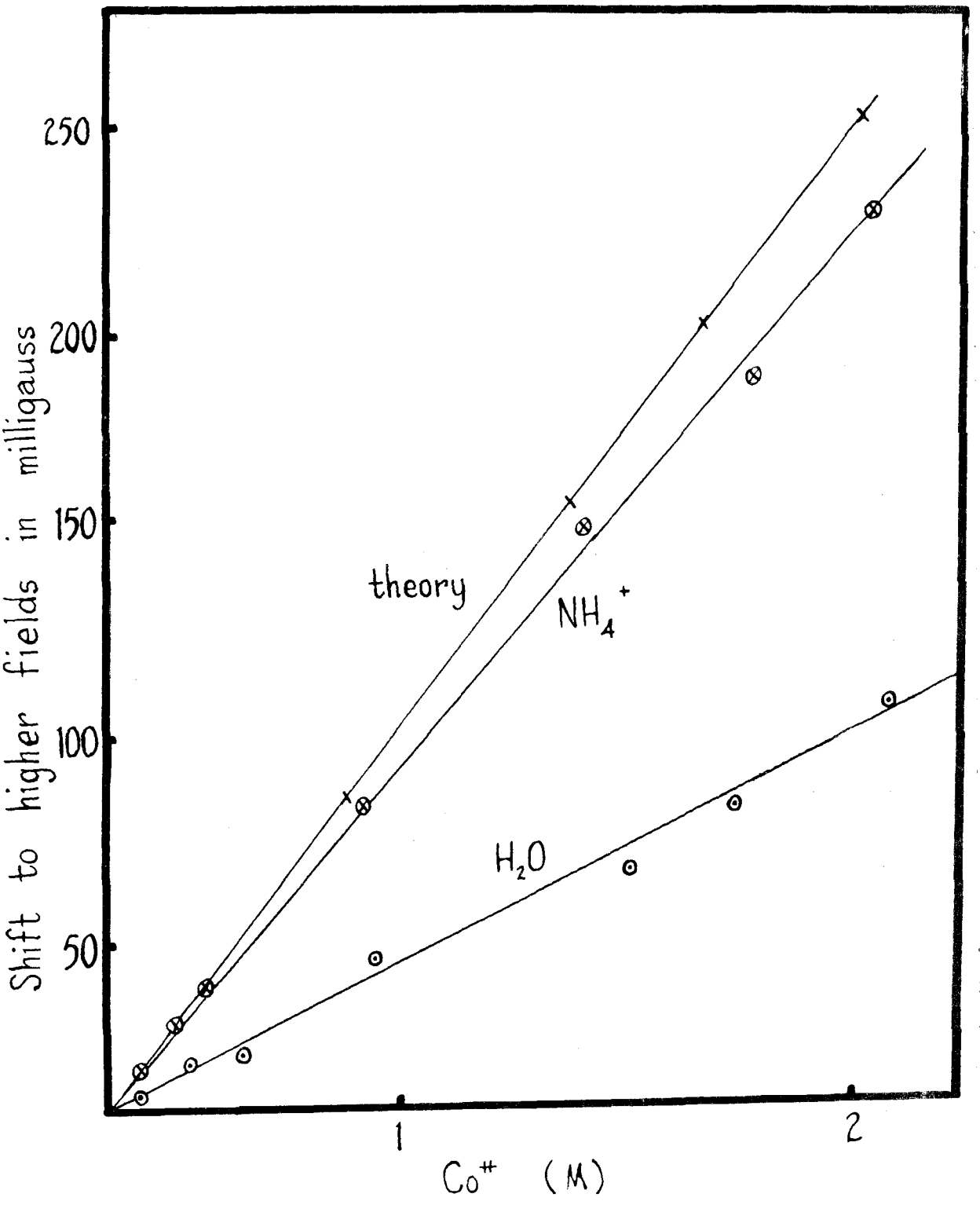

Fig. 7

Shifts in the NH_4^+-H_2O protons in aq. Co^{++} solution

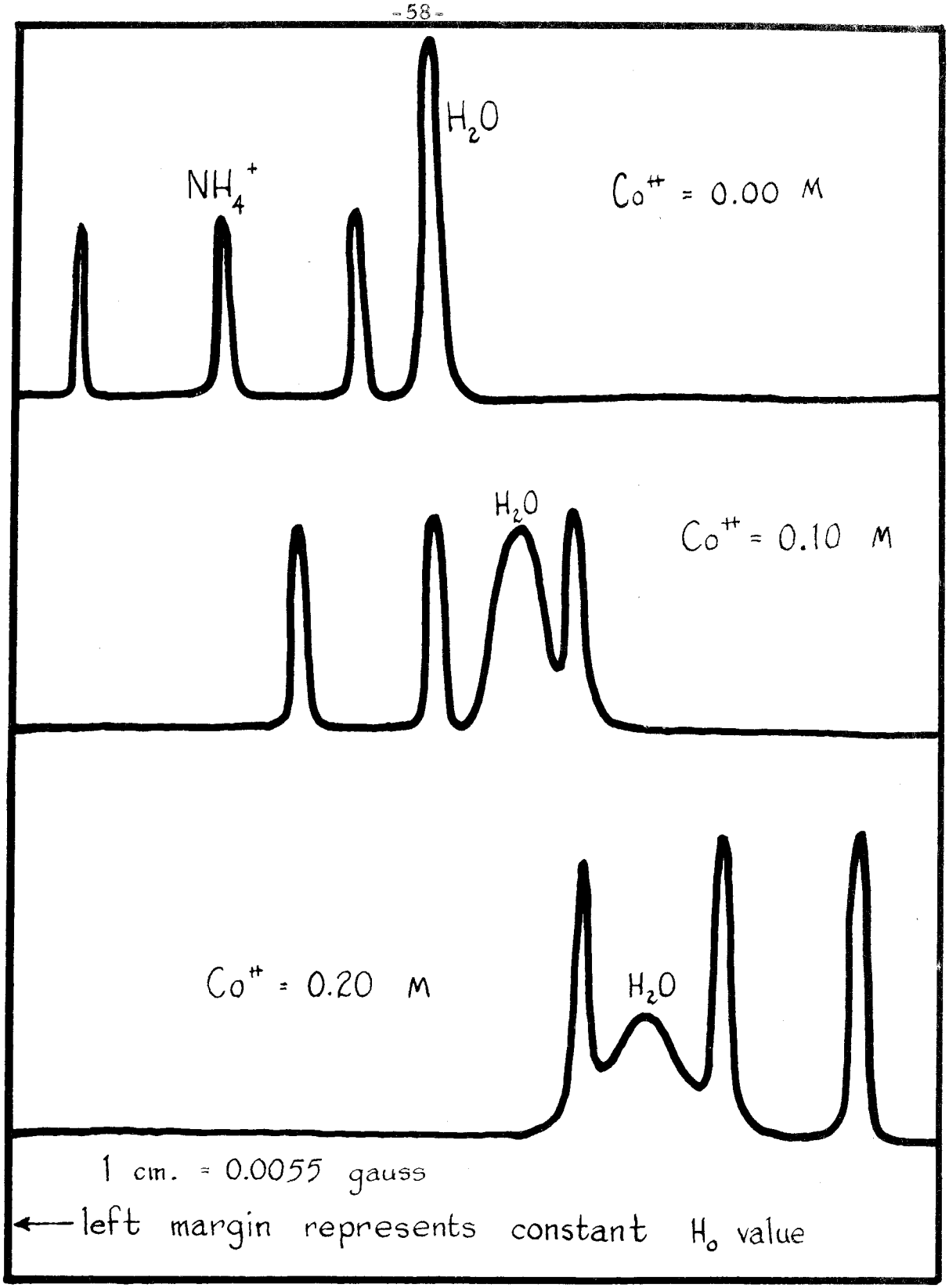

Fig. 8

Proton Spectra in the $NH_4^+ - H_2O$ System

It is interesting to observe the broadening of the two resonances. At 0.2M cobalt concentration, the water resonance line is perceptively broadened, while the width of the lines in the ammonium triplet has remained unchanged. Only at high cobalt concentrations, where the shift in the NH_4^+ protons deviates from the theoretical shift, does one see a perceptive broadening of the triplet. This is a good indication that the influence of the paramagnetic ion on the protons is dependent on the nearness of approach of the two.

Discussion

It is difficult from the above experimental data to distinguish between the effects of a hyperfine interaction and the anisotropy in causing the observed shifts. Both mechanisms tend to decrease the shifts caused by the change in the isotropic magnetic susceptibility in the system. Both mechanisms also depend on the proximity of the paramagnetic species to the resonating nuclei. The reason that no anomalous shift was found in the DPPH system is probably due to the fact that the species are so far apart, that no direct electron-nucleus interaction occurs. One would not expect an isotropic hyperfine interaction since there are no strong forces, such as electrostatic forces, which would tend to bring the species together. Therefore, on this basis, we can only conclude that there is not very much association between the free radical and the solvent in the DPPH solutions.

The observed shifts in the ammonium chloride system can also be explained by considering the type of molecular association which takes place in the solution. Since both the cobaltous ion and

the NH_4^+ ion are positively charged, they will tend to repel each other and thus decrease the effect of any type of interaction which depends on the proximity of the species. However, at high cobalt concentrations, the species are pushed closer together and the effect of some type of electron-nucleus interaction is observed. This interaction, in all probability, is due to a dipole-dipole coupling of the spins in the system. An isotropic hyperfine interaction is unlikely in the system, since it requires the species to be closer together.

On the other hand, the water molecules, due to their electrical dipole moments, are attracted to the positively charged cobaltous ion. In the solution, the Co^{++} is probably surrounded by six water molecules and one would expect the water protons to be greatly affected by the paramagnetic ion. However, the observed shifts, in this case, can be due either to the anisotropy of the hydrated cobaltous complex or to a hyperfine interaction between the water protons and the electrons of the cobaltous ion.

Conclusion

As was mentioned previously, it is difficult on the basis of the experiments performed to distinguish between the effects of a hyperfine interaction and the anisotropy in causing the observed shifts. Both mechanisms tend to decrease the shifts caused by the isotropic magnetic susceptibility in the system.

In some cases, as in the ferric fluoride system discussed previously, the hyperfine interaction is known to be the predominant mechanism, while in others, such as aqueous Cu^{++} solutions, the anisotropy is probably the major factor. In most cases there is probably a mixture of both effects.

REFERENCES

1. E. R. Andrew, Nuclear Magnetic Resonance. (Cambridge University Press, London, 1955).

2. D. J. E. Ingram, Spectroscopy at Radio and Microwave Frequencies. (Butterworth's Publications, London, 1955).

3. N. F. Ramsey, Nuclear Moments, (Wiley, New York, 1953).

4. J. E. Wertz, Chem. Revs. 55 829 (1955).

5. B. Bleaney, J. Phys. Chem. 57 508 (1953).

6. G. E. Pake, Solid State Physics, 2 1 (1957).

7. H. M. McConnell, Ann. Rev. Phys. Chem. 8 105 (1957).

8. F. Bloch, W. W. Hausen and M. Packard, Phys. Rev. 70 474 (1946).

9. E. M. Purcell, H. C. Torrey, and R. V. Pound, Phys. Rev. 69 37 (1946).

10. N. Bloembergen, E. M. Purcell and R. V. Pound, Phys. Rev. 73 679 (1948).

11. J. R. Zimmerman, J. Chem. Phys. 22 950 (1954).

12. I. Solomon, Phys. Rev. 99 559 (1955).

13. A. W. Nolle and L. O. Morgan, J. Chem. Phys. 26 642 (1957).

14. A. L. Bloom, J. Chem. Phys. 25 793 (1956).

15. N. Bloembergen, J. Chem. Phys. 27 572 (1957).

16. I. Solomon and N. Bloembergen, J. Chem. Phys. 25 261 (1956).

17. A. E. Martell and M. Calvin, Chemistry of the Metal Chelate Compounds (Prentice-Hall, New Jersey 1956) p. 537.

18. Chiarotti, Cristiani, Giulotto, and Lanzi, Nuovo Cimento, 12 519 (1954).

19. W. A. Anderson and J. J. Arnold, Phys. Rev. 101 511 (1956).

20. F. Bloch, Phys. Rev., 70 460 (1946).

REFERENCES (Cont'd)

21. M. Tinkham, R. Weinberg and A. Kip, Phys. Rev. 84 848 (1951).

22. T. X. England and E. E. Schneider, Phys. Rev. 17 221 (1951).

23. R. E. Connick and R. E. Poulson, J. A. C. S., 79, 5135 (1957).

24. C. A. Whitmer and R. T. Weidner, Phys. Rev. 84, 159 (1951).

25. R. T. Weider, P. R. Weiss, C. A. Whitmer, and D. R. Blosser, Phys. Rev., 76, 1727 (1949).

26. A. H. Cooke, Proc. Phys. Soc., A62, 269 (1949).

27. B. Bleaney and R. S. Trenan, Proc. Phys. Soc. A65 560 (1952).

28. H. W. Dodgen and G. K. Rollefson, J.A.C.S., 71, 2600 (1949).

29. Connick, Hepler, Hugus, Kury, Latimer, and Tsao, J.A.C.S., 78, 1827 (1956).

30. E. A. Swift, A System of Chemical Analysis (Prentice-Hall, New York, 1949) p. 299.

31. Private Communications.

32. G. W. Low, Jr. and E. H. Pryde, J.A.C.S., 61, 2237 (1942).

33. A. Babko and K. Kleiner, J. Gen. Chem. (U.S.S.R.) 17, 1259 (1947).

34. V. Jaccarino, R. G. Shulman and J. W. Stout, Phys. Rev. 106, 602 (1957).

35. R. G. Shulman and V. Jaccarino, Phys. Rev. 108, 1219 (1957).

36. W. Dickinson, Phys. Rev. 77 736 (1950).

APPENDIX

CALCULATION OF THE AVERAGE FIELDS IN REGIONS (1) AND (3) OF FIGURE 6

In the regions of interest the magnetic induction $\underline{B}$ can be related to a magnetic scalar potential Ω by the equation

$$\underline{B} = -\mu \nabla \Omega \tag{1}$$

The permeability, μ, is equal to $1 + 4\pi K_0$, where K_0 is the susceptibility.

The magnetic scalar potential Ω satisfies Laplace's Equation.

$$\nabla^2 \Omega = 0 \tag{2}$$

with the boundary conditions

$$\underline{B}_1 \cdot n = \underline{B}_2 \cdot n \tag{3}$$

$$\Omega_1 = \Omega_2 \tag{4}$$

and

$$\frac{1}{\mu_1} \underline{B} \times n = \frac{1}{\mu_2} \underline{B} \times n \tag{5}$$

where $\underline{n}$ is a unit vector normal to the boundary.

The solution of equation 2 in cylindrical coordinates is:

$$\Omega = \sum_{n=0}^{\infty} \Theta_n R_n \tag{6}$$

where

$$\Theta_0 = A_0 \theta + B_0 \tag{7}$$

$$R_0 = C_0 \ln r + D_0 \tag{8}$$

and for $n \gg 1$

$$\Theta_n = A_n \cos n\theta + B_n \sin n\theta \tag{9}$$

$$R_n = C_n r^n + D_n r^n \tag{10}$$

From equation 4 we can write

$$\begin{aligned} \Omega_1(r=a) &= \Omega_2(r=a) \\ \Omega_2(r=b) &= \Omega_3(r=b) \\ \Omega_3(r=c) &= \Omega_4(r=c) \\ \Omega_4(r=d) &= \Omega_5(r=d) \end{aligned} \tag{11}$$

where Ω_i is the magnetic scalar potential in region (i) of figure 6.

Then

$$\Omega_1 = \sum_{n=0}^{\infty} \Theta_n^{(1)} R_n^{(1)} \tag{12}$$

where

$$\Theta_n^{(1)} = A_n^{(1)} \cos n\theta + B_n^{(1)} \sin n\theta \tag{13}$$

and

$$R_n^{(1)} = C_n^{(1)} r^n + D_n r^{-n} \quad \text{for } n \geq 1 \tag{14}$$

Since all the Ω's must be symmetric about the z-axis the following relations must hold.

$$A_0^{(1)} = A_0^{(2)} = A_0^{(3)} = A_0^{(4)} = A_0^{(5)} = 0 \tag{15}$$

and for $n > 0$

$$B_n^{(1)} = B_n^{(2)} = B_n^{(3)} = B_n^{(4)} = B_n^{(5)} = 0 \tag{16}$$

The general expression for Ω (cf. equation 6) can be written as

$$\Omega = \sum_{n=0}^{\infty} \Theta_n R_n$$

where $\Theta_0 = 1$

AND for $n \geq 1$

$$\Theta_n = \cos n\theta \tag{17}$$

$$R_n = C_n r^n + D_n r^{-n} \tag{18}$$

AND for $n = 0$

$$R_0 = C_0 \ln r + D_0 \tag{19}$$

By using the relation

$$\int_0^{2\pi} \cos n\theta \cos m\theta \, d\theta = 0 \quad \text{if } m \neq n \tag{20}$$

the boundary conditions given by equation 11 become

$$\begin{aligned} R_n^{(1)}(r=a) &= R_n^{(2)}(r=a) \\ R_n^{(2)}(r=b) &= R_n^{(3)}(r=b) \\ R_n^{(3)}(r=c) &= R_n^{(4)}(r=c) \\ R_n^{(4)}(r=d) &= R_n^{(5)}(r=d) \end{aligned} \tag{21}$$

If equation 1 is expanded in terms of the boundary conditions equations 5 and 21, the following equations are obtained.

$$\begin{aligned} \mu_1 \frac{dR_n^{(1)}}{dr}\bigg|_{r=a} &= \mu_2 \frac{dR_n^{(2)}}{dr}\bigg|_{r=a} \\ \mu_2 \frac{dR_n^{(2)}}{dr}\bigg|_{r=b} &= \mu_3 \frac{dR_n^{(3)}}{dr}\bigg|_{r=b} \end{aligned} \tag{22}$$

$$\mu_3 \left.\frac{dR_n^{(3)}}{dr}\right|_{r=c} = \mu_2 \left.\frac{dR_n^{(4)}}{dr}\right|_{r=c}$$

$$\mu_2 \left.\frac{dR_n^{(4)}}{dr}\right|_{r=d} = \left.\frac{dR_n^{(5)}}{dr}\right|_{r=d} \qquad (22)\ \text{(Cont'd)}$$

where we have assumed μ_5, the permeability of air, to be unity. The only non-zero solution for these equations is for n = 1.

Then, using equation 19, the boundary conditions equations 21 and 22 become

$$\begin{aligned}
C_1 a + D_1 a^{-1} &= C_2 a + D_2 a^{-1} && \text{(I)}\\
C_2 b + D_2 b^{-1} &= C_3 b + D_3 b^{-1} && \text{(II)}\\
C_3 c + D_3 c^{-1} &= C_4 c + D_4 c^{-1} && \text{(III)}\\
C_4 d + D_4 d^{-1} &= C_5 d + D_5 d^{-1} && \text{(IV)}
\end{aligned} \qquad (23)$$

and

$$\begin{aligned}
\mu_1 C_1 + \mu_1 D_1 a^{-2} &= \mu_2 (C_2 - D_2 a^{-2}) && \text{(V)}\\
\mu_2 (C_2 - D_2 b^{-2}) &= \mu_3 (C_3 - D_3 b^{-2}) && \text{(VI)}\\
\mu_3 (C_3 - D_3 c^{-2}) &= \mu_2 (C_4 - D_4 c^{-2}) && \text{(VII)}\\
\mu_2 (C_4 - D_4 d^{-2}) &= C_5 - D_5 d^{-2} && \text{(VIII)}
\end{aligned} \qquad (24)$$

where the subscriptsrefer to the particular region.

Since Ω must be finite at r = 0, we must have $D_1 = 0$. At $r = \infty$ and $\theta = 0$ the field must be H_o, then $C_5 = -H_o$.

Thus we have eight equations in eight unknowns which can be solved for the coefficients, C_1, C_2, D_2, C_3, D_3, C_4, and D_4. We are primarily concerned with the coefficients C_1, C_3, and D_3 since the magnetic induction in region (3), i.e., the annulus, is given by

$$B^{2(3)} = B_x^{2(3)} + B_z^{2(3)} \tag{25}$$

with a similar equation for region (1).

Then, from equation 1

$$\begin{aligned} B_z^{(i)} &= -\mu_i \frac{d}{dz} \Omega_i \qquad \text{WHERE } i = 1 \text{ or } 3 \\ &= -\mu_i \frac{d}{dz} (C_i r + D_i r^{-1}) \cos\theta \qquad (26) \\ &= -\mu_i \left[C_i + D_i \frac{(\sin^2\theta - \cos^2\theta)}{r^2} \right] \end{aligned}$$

Similarly,

$$B_x^{(i)} = -\mu_i \frac{d}{dx} \Omega_i = \frac{\mu_i \, 2 \sin\theta \cos\theta \, D_i}{r^2} \tag{27}$$

Using I, II, V, and VI of equations 23 and 24 to get an expression involving C_1, C_3, and D_3 and remembering that $D_1 = 0$, we first eliminate D_2 between I and V, and between II and VI.

From I and V

$$D_2 = C_1 a^2 - C_2 a^2$$

and

$$D_2 = C_2 a^2 - \mu_1/\mu_2 C_1 a^2$$

Combining, we have:

$$C_2 = \frac{C_1 (\mu_1 + \mu_2)}{2\mu_2} \qquad \text{(I, V)}$$

From II and VI we get

$$D_2 = C_3 b^2 + D_3 - C_2 b^2$$

and

$$D_2 = C_2 b^2 - (\mu_3/\mu_2) b^2 C_3 + (\mu_3/\mu_2) D_3$$

Thus

$$C_2 = C_3 (\mu_2 + \mu_3/2\mu_2) + D_3 b^{-2} (\mu_2 - \mu_3/2\mu_2^2) \quad \text{(II, VI)}$$

Equating (I, V) and (II, VI) we get the expression for C_1 in terms of C_3 and D_3.

$$C_1 = C_3 \left(\frac{\mu_2+\mu_3}{\mu_1+\mu_2}\right) + D_3 b^{-2} \left(\frac{\mu_2-\mu_3}{\mu_1+\mu_2}\right) \quad \text{(IX)}$$

To get an expression for C_3 and D_3 in terms of H_o, we solve IV and VIII for D_5.

$$D_5 = C_4 d^2 + D_4 - C_5 d^2$$

$$D_5 = C_5 d^2 - \mu_2 (C_4 d^2 - D_4)$$

Solving these two equations for C_4, we have

$$C_4 = \frac{2C_5}{1+\mu_2} - \frac{D_4}{d^2}\left(\frac{1-\mu_2}{1+\mu_2}\right) \quad \text{(X)}$$

Eliminating C_4 from III, VII and X we get

$$C_4 = C_3 + D_3 c^{-2} - D_4 c^{-2}$$

$$C_4 = \mu_3/\mu_2 (C_3 - D_3 c^{-2}) + D_4 c^{-2}$$

$$C_3 + D_3 c^{-2} - D_4 c^{-2} = \mu_3/\mu_2 (C_3 - D_3 c^{-2}) + D_4 c^{-2} \quad \text{(XI)}$$

$$C_3 + D_3 c^{-2} - D_4 c^{-2} = \frac{2C_5}{1+\mu_5} - \frac{D_4}{d^2}\left(\frac{1-\mu_2}{1+\mu_2}\right) \quad \text{(XII)}$$

If we solve these equations for D_4, we get

$$D_4 = C_3 \frac{c^2}{2}\left(\frac{\mu_2-\mu_3}{\mu_2}\right) + \frac{D_3}{2}\left(\frac{\mu_2+\mu_3}{\mu_2}\right)$$

and from XII

$$D_4 = \frac{C_3 c^2(1+\mu_2) + D_3(1-\mu_2) - 2C_5c^2}{1+\mu_2-(c/d)^2(1-\mu_2)}$$

Equating the two we have

$$\frac{C_3c^2(\mu_2-\mu_3)}{2\mu_2} + \frac{D_3(\mu_2+\mu_3)}{2\mu_2} = \frac{C_3c^2(1+\mu_2)+D_3(1-\mu_2)-2C_5c^2}{1+\mu_2-(c/d)^2(1-\mu_2)} \quad \text{(XIII)}$$

We can now get another equation which expresses C_3 and D_3 in terms of C_5.

If we eliminate C_1 from equations I and V, we get

$$C_1 = C_2 + D_2a^{-2}$$

$$C_1 = (\mu_2/\mu_1)(C_2 - D_2a^{-2})$$

Then,

$$C_2 + D_2a^{-2} = (\mu_2/\mu_1)C_2 - (\mu_2/\mu_1)D_2a^{-2}$$

or

$$C_2 = -D_2a^{-2}\left(\frac{\mu_1+\mu_2}{\mu_1-\mu_2}\right) \quad \text{(XIV)}$$

C_2 can be eliminated from II, VI and XIV.

$$C_2 = C_3 + D_3b^{-2} - D_2b^{-2} \quad \text{(II)}$$

$$C_2 = (\mu_3/\mu_2)(C_3 - D_3b^{-2}) + D_2b^{-2} \quad \text{(VI)}$$

Combining II and VI

$$C_3 + D_3 b^{-2} - D_2 b^{-2} = (\mu_3/\mu_2)(C_3 - D_3 b^{-2}) + D_2 b^{-2}$$

$$D_2 = \frac{C_3 b^2}{2\mu_2}(\mu_2 - \mu_3) + \frac{D_3}{2\mu_2}(\mu_2 + \mu_3) \qquad (XV)$$

Solving II and XIV for D_2, we get

$$D_2 = \frac{(C_3 b^2 + D_3)(\mu_1 - \mu_2)}{\mu_1 - \mu_2 - (b/a)^2(\mu_1 + \mu_2)} \qquad (XVI)$$

By equating XV and XVI we have a second equation containing only the unknowns C_3 and D_3.

$$\frac{C_3 b^2}{2\mu_2}(\mu_2 - \mu_3) + \frac{D_3}{2\mu_2}(\mu_2 + \mu_3) = \frac{(C_3 b^2 + D_3)(\mu_1 - \mu_2)}{\mu_1 - \mu_2 - (\mu_1 + \mu_2)(b/a)^2}$$

Expressing D_3 in terms of C_3 and C_5, we have, from XIII

$$D_3 = \frac{C_3 c^2[\mu_2(1+\mu_2) + \mu_2(1-\mu_2)(c/d)^2 + \mu_3(1+\mu_2) - \mu_3(1-\mu_2)(c/d)^2] - 4C_5 c^2 \mu_2}{\mu_3(1+\mu_2) - \mu_3(1-\mu_2)(c/d)^2 - \mu_2(1-\mu_2)(c/d)^2 - \mu_2(1+\mu_2)}$$

$$= - \frac{C_3[(\mu_2+\mu_3)(1+\mu_2) + (\mu_2-\mu_3)(1-\mu_2)(c/d)^2] - 4C_5\mu_2}{(\mu_2-\mu_3)(1+\mu_2)c^{-2} + (\mu_2+\mu_3)(1-\mu_2)d^{-2}} \qquad (XVIII)$$

and from XVII

$$D_3 = \frac{C_3 b^2[2(\mu_1-\mu_2)\mu_2 - (\mu_2-\mu_3)(\mu_1-\mu_2-(\mu_1+\mu_2)(b/a)^2)]}{(\mu_2+\mu_3)[\mu_1-\mu_2-(\mu_1+\mu_2)(b/a)^2] - 2\mu_2(\mu_1-\mu_2)} \qquad (XIX)$$

$$= - \frac{C_3 b^2[(\mu_2+\mu_3)(\mu_1-\mu_2) + (\mu_2-\mu_3)(\mu_1+\mu_2)(b/a)^2]}{(\mu_2-\mu_3)(\mu_1-\mu_2) + (\mu_1+\mu_2)(\mu_2+\mu_3)(b/a)^2}$$

$$= - \frac{C_3[(\mu_2+\mu_3)(\mu_1-\mu_2) + (\mu_2-\mu_3)(\mu_1+\mu_2)(b/a)^2]}{(\mu_2-\mu_3)(\mu_1-\mu_2)b^{-2} + (\mu_1+\mu_2)(\mu_2+\mu_3)a^{-2}}$$

Let

$$\alpha = (\mu_2+\mu_3)(\mu_1-\mu_2) + (\mu_2-\mu_3)(\mu_1+\mu_2)(b/a)^2$$

$$\beta = (\mu_2-\mu_3)(\mu_1-\mu_2)b^{-2} + (\mu_1+\mu_2)(\mu_2+\mu_3)a^{-2}$$

$$\gamma = (\mu_2+\mu_3)(1+\mu_2) + (\mu_2-\mu_3)(1-\mu_2)(c/d)^2$$

$$\delta = (\mu_2-\mu_3)(1+\mu_2)c^{-2} + (\mu_2+\mu_3)(1-\mu_2)d^{-2}$$

Then, equating XVIII and XIX

$$-C_3\frac{\alpha}{\beta} = +\frac{-C_3\gamma + 4C_5\mu_2}{\delta}$$

$$C_3\left(\frac{-\alpha}{\beta}+\frac{\gamma}{\delta}\right) = \frac{4C_5\mu_2}{\delta}$$

$$C_3\frac{(\gamma\beta-\alpha\delta)}{\beta\delta} = \frac{4C_5\mu_2}{\delta} \qquad (28)$$

$$C_3 = \frac{4C_5\mu_2\beta}{\gamma\beta-\alpha\delta} = -\frac{4H_0\mu_2\beta}{\gamma\beta-\alpha\delta}$$

from XIX

$$D_3 = -C_3\frac{\alpha}{\beta} = -\frac{4C_5\mu_2\alpha}{\gamma\beta-\alpha\delta} \qquad (28)'$$

Expanding the denominator

$$\gamma\beta = (\mu_2^2-\mu_3^2)(\mu_1-\mu_2+\mu_1\mu_2-\mu_2^2)b^{-2}$$

$$+[(\mu_2^2+\mu_3^2)(\mu_1+\mu_2+\mu_1\mu_2+\mu_2^2)+2\mu_3\mu_2(\mu_2+\mu_1\mu_2+\mu_1\mu_2)]a^{-2}$$

$$+(\mu_2-\mu_3)^2(\mu_1-\mu_2+\mu_2^2-\mu_1\mu_3)(c/d)^2b^{-2}$$

$$+(\mu_2^2-\mu_3^2)(\mu_1+\mu_2-\mu_1\mu_2-\mu_2^2)(c/d)^2a^{-2} \qquad (29)$$

and noting that

$$\mu_1 = 1 + 4\pi\kappa_{b1}\,, \qquad \mu_2 = 1 + 4\pi\kappa_{b2}\,, \quad \text{etc.}$$

$$\mu_i^2 \cong 1 + 8\pi\kappa_{bi} \qquad \mu_i\mu_j \cong 1 + 4\pi(\kappa_{bi} + \kappa_{bj})$$

$$\mu_i^2 + \mu_j^2 = 2 + 8\pi(\kappa_{bi} + \kappa_{bj}) = 2\mu_i\mu_j$$

$$\mu_i + \mu_j = 2 + 4\pi(\kappa_{bi} + \kappa_{bj})$$

$$\mu_i^2 - \mu_j^2 = 8\pi(\kappa_{bi} - \kappa_{bj})$$

$$\mu_i - \mu_j = 4\pi(\kappa_{bi} - \kappa_{bj})$$

we can write the product in terms of the κ_b's. Since the susceptibilities are of the order of 10^{-6}, second order terms can be neglected.

In terms of the susceptibilities equation 29 becomes

$$\gamma\beta = 64\pi^2(\kappa_{b2} - \kappa_{b3})(\kappa_{b1} - \kappa_{b2})b^{-2} + 16[1 + 2\pi(\kappa_{b1} + 2\kappa_{b2}) + 4\pi(\kappa_{b2} + \kappa_{b3})]a^{-2}$$

$$+ 16[1 + 2\pi(\kappa_{b1} + 2\kappa_{b2}) + 4\pi(\kappa_{b2} + \kappa_{b3})]a^{-2}$$

$$+ 64\pi^3(\kappa_{b2}^2 - \kappa_{b3}^2)(\kappa_{b2} - \kappa_{b3})(c/d)^2 b^{-2} - 64\pi^2\kappa_{b2}(\kappa_{b2} - \kappa_{b3})$$

$$\cong \quad 0 \quad + 16[1 + 2\pi\kappa_1 + 8\pi\kappa_{b2} + 4\pi\kappa_{b3}]a^{-2} + 0 + 0$$

Similarly, $\alpha\delta$ can be expressed in terms of the susceptibilities.

$$\alpha\delta = [\mu_1\mu_2(\mu_1+\mu_1\mu_2-\mu_1\mu_3+2\mu_2\mu_3-\mu_3^2-\mu_2+2\mu_3-\mu_2^2)$$

$$+\mu_3(-\mu_1^2-\mu_1\mu_3-\mu_2^2+\mu_2\mu_3-\mu_2^3+\mu_2^2\mu_3)]c^{-2}$$

$$+[\mu_1\mu_2(\mu_1-\mu_1\mu_2-\mu_1\mu_3-\mu_3^2-\mu_2+\mu_2^2)+\mu_1\mu_3(\mu_1+\mu_3)$$

$$+\mu_2\mu_3(-\mu_2-\mu_3+\mu_2^2+\mu_2\mu_3]d^{-2}$$

$$+(\mu_2^2-\mu_3^2)(\mu_1-\mu_1\mu_2+\mu_2-\mu_2^2)(b/a)^2d^{-2}$$

$$+[(\mu_2-\mu_3)^2(\mu_2+\mu_2^2)-2\mu_1\mu_3(\mu_1+\mu_2)^2+(\mu_2^2+\mu_3^2)(\mu_3+\mu_1\mu_2)](b/a)^2c^{-2}$$

$$=[(1+4\pi(K_{b1}+K_{b2}))(2+8\pi K_{b3})+(1+4\pi K_{b3})(-2-4\pi(K_{b1}+4\pi K_{b2}))]c^{-2}$$

$$+[(1+4\pi(K_{b1}+K_{b2}))(-2-4\pi K_{b1}-12\pi K_{b3})+(1+4\pi(K_{b1}+K_{b3}))(2+4\pi(K_{b1}+K_{b3}))$$

$$+8\pi K_{b2}(1+4\pi(K_{b2}+K_{b3}))]d^{-2}$$

$$+[(1+8\pi K_{b2}-1-8\pi K_{b3})(1+4\pi K_{b1}-1-4\pi(K_{b1}+K_{b2})+1+4\pi K_{b2}-1-8\pi K_{b2})](b/a)^2d^{-2}$$

$$+[(1+4\pi K_{b2}-1-4\pi K_{b3})^2(1+4\pi K_{b2}+1+8\pi K_{b2})$$

$$-2(1+4\pi(K_{b1}+K_{b3}))(1+4\pi K_{b2}+1+8\pi K_{b2})](b/a)^2c^{-2}$$

$$+[(1+8\pi K_{b2}+1+8\pi K_{b3})(1+4\pi K_{b1}+1+4\pi(K_{b1}+K_{b2})](b/a)^2c^{-2}$$

$$\cong \quad 0+0+0+0=0$$

which shows that, to a first approximation, $\alpha\delta$ can be neglected with respect to $\beta\gamma$

Rewriting equations 28 and 28', we have

$$C_3 = -\frac{4H_0\mu_2\beta}{\beta\gamma} = -\frac{4H_0\mu_2}{\gamma} \tag{30}$$

$$D_3 = \frac{4H_0\mu_2\alpha}{\beta\gamma} \tag{31}$$

From equations 25, 26, and 27, the magnetic induction in region (3) is

$$B^{2(3)} = B_x^{2(3)} + B_z^{2(3)} \tag{32}$$

$$B^{2(3)} = \frac{4\mu_3^2 \sin^2\theta\cos^2\theta D_3^2}{r^4} + \mu_3^2\left[C_3^2 + 2C_3D_3(\sin^2\theta - \cos^2\theta) + \frac{D_3^2}{r^4}(\sin^4\theta - 2\cos^2\theta\sin^2\theta + \cos^4\theta)\right]$$

Since $\sin^4\theta + \cos^4\theta = 1 - 2\cos^2\theta$, the last term in the brackets becomes

$$\frac{D_3}{r^4}\left[1 - 4\cos^2\theta\sin^2\theta\right]$$

The last term in this expression cancels the first term in equation 32 and we are left with

$$B^{2(3)} = \mu_3^2\left[C_3^2 + 2C_3D_3\left(\frac{\sin^2\theta - \cos^2\theta}{r^2}\right) + \frac{D_3^2}{r^4}\right] \tag{33}$$

If we let

$$C_3 = H_0 e \quad \text{and} \quad \frac{D_3}{r^2} = H_0 f \tag{34}$$

equation 33 can be written as

$$B^{2(3)} = \mu_3^2 H_0^2\left[e^2 + 2ef(2\sin^2\theta - 1) + f^2\right]$$

or since $\underline{B} = \mu\underline{H}$

$$H_3 = H_0[e^2 - 2ef + f^2 + 4ef\sin^2\theta]^{1/2}$$

$$= H_0[(e-f)^2 + 4ef\sin^2\theta]^{1/2}$$

$$= H_0(e-f)\left[1 + \frac{4ef\sin^2\theta}{(e-f)^2}\right]^{1/2} \qquad (35)$$

Expanding the square root,

$$H_3 = H_0(e-f)\left[1 + \frac{2ef\sin^2\theta}{(e-f)^2} - \frac{2e^2f^2\sin^4\theta}{(e-f)^4}\right]$$

where only the first three terms are kept.

To get the average field in region (3) we must average the value of H_3 over all orientations of the angle θ from 0 to π

$$\langle H_3\rangle = \frac{\int_0^\pi H_3 d\theta}{\int_0^\pi d\theta} = \frac{H_0(e-f)}{\pi}\int_0^\pi\left[1 + \frac{2ef\sin^2\theta}{(e-f)^2} - \frac{2e^2f^2\sin^4\theta}{(e-f)^4}\right]d\theta$$

$$= \frac{H_0(e-f)}{\pi}\left[\pi + \frac{ef\pi}{(e-f)^2} - \frac{3}{4}\frac{e^2f^2\pi}{(e-f)^4}\right]$$

$$= H_0(e-f)\left[1 + \frac{ef}{(e-f)^2} - \frac{3e^2f^2}{4(e-f)^4}\right] \qquad (36)$$

From equations 30 and 34

$$e = \frac{C_3}{H_0} = -\frac{4\mu_2}{\gamma}$$

$$f = \frac{D_3}{H_0\ell^2} = \frac{4\mu_2\alpha}{\gamma\beta\ell^2}$$

In terms of the susceptibilities

$$\alpha = 8\pi\left[\kappa_1 - \kappa_2 + (b/a)^2\kappa_2 - (b/a)^2\kappa_3\right]$$

$$\gamma = 4\left[1 + 4\pi\kappa_2 + 2\pi\kappa_3\right]$$

If the last term in equation 36 is neglected, we can write

$$\begin{aligned}\langle H_3\rangle &= H_0(e-f)\left[1 + \frac{ef}{(e-f)^2}\right] \\ &= -H_0\left[1 + 2\pi\kappa_1(a/r)^2 - 2\pi\kappa_2(a/r)^2 + 2\pi\kappa_2(b/r)^2 - 2\pi\kappa_3 - 2\pi\kappa_3(b/r)^2\right] \\ &\quad \times\left[1 - 2\pi\kappa_1(a/r)^2 + 2\pi\kappa_2(a/r)^2 - 2\pi\kappa_2(b/r)^2 + 2\pi\kappa_3(b/a)^2\right] \\ &\cong + H_0(1 - 2\pi\kappa_3)\end{aligned} \tag{37}$$

where as before second order terms have been neglected.

To obtain the expression for the field in region (1), we again use equations 25, 26, and 27.

$$B^{2(1)} = B_x^{2(1)} + B_z^{2(1)}$$

but

$$B_x^{(1)} = \frac{\mu_1 2\sin\theta\cos\theta D_1}{r^2} = 0 \quad \text{since } D_1 = 0$$

Then,

$$B^{2(1)} = B_z^{2(1)} = \mu_1^2 C_1^2$$

or

$$H_1 = -C_1$$

From IX

$$C_1 = C_3\frac{(\mu_2+\mu_3)}{\mu_1+\mu_2} + D_3 b^{-2}\frac{(\mu_2-\mu_3)}{\mu_1+\mu_2}$$

In terms of the susceptibilities this becomes

$$C_1 = C_3\left(\frac{2+4\pi K_2+4\pi K_3}{2+4\pi K_1+4\pi K_2}\right) + D_3 b^{-2}\left(\frac{4\pi K_2-4\pi K_3}{2+4\pi K_1+4\pi K_2}\right)$$

$$= C_3(1+2\pi K_2+2\pi K_3)(1-2\pi K_1-2\pi K_2)$$

$$+ D_2 b^{-2}(2\pi K_2-2\pi K_3)(1-2\pi K_1-2\pi K_2)$$

$$= C_3(1-2\pi K_1+2\pi K_3) + D_3 b^{-2}(2\pi K_2-2\pi K_3)$$

Substituting the values of C_3 and D_3 from equations 30 and 31

$$C_1 = -16 H_0 M_2 a^{-2}\left[\frac{1+2\pi K_1+4\pi K_2+2\pi K_3}{16a^{-2}(1-2\pi K_1-8\pi K_2-4\pi K_3}\right]\left[1-2\pi K_1+2\pi K_3\right]$$

$$+32\pi M_2 \frac{[K_1-K_2+(b/a)^2 K_2-(b/a)^2 K_3][2\pi K_2-2\pi K_3]}{16a^{-2}[1-2\pi K_1-8\pi K_2-4\pi K_3]}$$

where the susceptibilities have been used.

If second order terms are neglected

$$C_1 = -H_0(1-2\pi K_1)$$

and

$$H_1 = -C_1 = H_0(1-2\pi K_1) \tag{38}$$

The term $-2\pi K$ which appears in equations 37 and 38 is just the contribution to the field due to the demagnetization in the sample.

To get the total average fields in regions (1) and (3), one must add to the above expressions the Lorentz field which is $\frac{4\pi}{3} H_0 K$

Then,

$$\langle H_3 \rangle = H_0(1-2\pi K_3+\frac{4\pi}{3}K_3) = H_0(1-\frac{2\pi}{3}K_3) \tag{39}$$

$$\langle H_1 \rangle = H_0(1-2\pi K_1+\frac{4\pi}{3}K_1) = H_0(1-\frac{2\pi}{3}K_1) \tag{40}$$

These are the equations quoted in the text.

PART II

KINETICS OF THE FERROUS ION-OXYGEN REACTION IN ACIDIC PHOSPHATE-PYROPHOSPHATE SOLUTIONS

This section consists of a paper published with

Professor Norman Davidson

in the Journal of the American Chemical Society

79-82

In the original copy of this thesis the pages indicated above contain the text of a published article:

"Kinetics of the Ferrous Iron-Oxygen Reaction in Acidic Phosphate-Pyrophosphate Solutions"

by

James King and Norman Davidson

in the

Journal of the American Chemical Society

Vol. 80, pp. 1542-1545 (1958)

[Reprinted from the Journal of the American Chemical Society, **80**, 1542 (1958).]
Copyright 1958 by the American Chemical Society and reprinted by permission of the copyright owner.

[CONTRIBUTION NO. 2260 FROM THE GATES AND CRELLIN LABORATORIES OF CHEMISTRY, CALIFORNIA INSTITUTE OF TECHNOLOGY]

Kinetics of the Ferrous Iron–Oxygen Reaction in Acidic Phosphate–Pyrophosphate Solutions

BY JAMES KING AND NORMAN DAVIDSON[1]

RECEIVED OCTOBER 15, 1957

The rate law for the ferrous iron–oxygen reaction in acid solutions (pH ~1–2) containing phosphate and pyrophosphate anions is $-d(Fe^{++})/dt = k_1(Fe^{++})(H_2PO_4^-)^2P_{O_2} + k_2(Fe^{++})(H_2P_2O_7^=)P_{O_2}$ where $k_1 = 1.08(\pm 0.06) \times 10^{-3}$ atm.$^{-1}$ mole^{-2} liter^2 sec.$^{-1}$ and $k_2 = 2.13(\pm 0.05) \times 10^{-2}$ atm.$^{-1}$ mole^{-1} liter sec.$^{-1}$ at 30° (μ = 1.0–1.1 mole/liter, $NaClO_4$). The activation energies are $\Delta H_1^* = 21(\pm 1)$ and $\Delta H_2^* = 6(\pm 1)$ kcal. The rate law and the values of k_1 and k_2 both show that $H_2P_2O_7^=$ and $H_2PO_4^-$ are independent catalysts and that the unusual quadratic dependence on $(H_2PO_4^-)$ is not due to the equilibrium $2H_2PO_4^- \rightleftarrows H_2P_2O_7^= + H_2O$. The mechanism of the reaction presumably involves as the rate-determining step either the one electron transfer process $Fe^{II} + O_2 \rightarrow Fe^{III} + O_2^-$ or the two-electron process $Fe^{II} + O_2 \rightarrow Fe^{IV} + O_2^=$, with iron in the transition state stabilized by the complexing phosphorous anions.

Cher and Davidson[2] found that the rate law for the oxygenation of Fe^{II} in phosphoric acid solution is $-d(Fe^{++})/dt = k_1(Fe^{++})P_{O_2}(H_2PO_4^-)^2$. The quadratic dependence on $(H_2PO_4^-)$ is somewhat

(1) We are indebted to the Atomic Energy Commission for support of this research under Contract AT(11-1)-188; and to the Danforth Foundation and the General Education Board for fellowships to one of us (J.K.). This paper was presented in part at the 129th National Meeting of the A. C. S., Dallas, April, 1956.

(2) M. Cher and N. Davidson, THIS JOURNAL, **77**, 793 (1955).

unusual. A linear dependence would be expected in view of: (a) general experience with this kind of reaction; (b) the reported first-order dependence on (F^-) for the fluoride catalysis of the Fe^{II}, O_2 reaction[3]; and (c) the reported fact that the first complex formed between Fe^{+++} and phosphate anions in acid solution contains one phosphate per iron, being either $FeHPO_4^+$ or $FeH_2PO_4^{++}$.[4,5] The quadratic dependence on dihydrogen phosphate concentration would be explained if the actual catalyst were dihydrogen pyrophosphate, formed in equilibrium amounts according to the reaction

$$2H_2PO_4^- \rightleftharpoons H_2P_2O_7^= + H_2O$$

This hypothesis and a general interest in the effects of pyrophosphate stimulated the present work.

Spoehr[6] and Smith and Spoehr[7] have reported that there is an accelerating influence of pyrophosphate on the Fe^{II}–O_2 reaction. The latter authors claim that the rate law is $-d(Fe^{II})/dt = k(Fe^{II})(O_2)$; but a later study[8] of the effects of stirring indicates that the reaction rate was diffusion controlled under the conditions employed.

Other references to studies of the Fe^{II}–O_2 reaction in various media are given in another paper from this Laboratory.[9]

Experimental

The rate of O_2 uptake was measured by a manometric method with a Warburg apparatus, as described previously.[2] The apparatus was well thermostated and had provisions for vigorous shaking of the reaction mixtures.

Reagent grade ferrous ammonium sulfate and sodium hydroxide were used. Sodium perchlorate, for maintaining ionic strength, was prepared by neutralization of known amounts of 85% perchloric acid with sodium hydroxide. The commercial redistilled water used in the initial experiments was found to contain trace amounts of copper. For all the results reported here, water was prepared by redistilling the commercial distilled water in a Pyrex, electrically heated still, to remove the traces of copper. The necessary precautions were taken to exclude dust from the vessels and each reaction vessel was pre-rinsed with the redistilled water. The desired H_3PO_4–$H_2PO_4^-$ buffer solutions were prepared by the appropriate neutralization of reagent grade phosphoric acid with standard sodium hydroxide solution. Pyrophosphate solutions were prepared from weighed quantities of reagent grade $Na_4P_2O_7 \cdot 10H_2O$ and checked acidimetrically.

The procedure was to dissolve separately ferrous ammonium sulfate and sodium pyrophosphate in phosphate buffer. Corrections of the H_3PO_4–$H_2PO_4^-$ ratio were made for the effects due to the conversion of $P_2O_7^{-4}$ to $H_2P_2O_7^{-2}$ and $H_3P_2O_7^{-1}$. Varying amounts of the two solutions were placed in the 15-ml. reaction flasks, the total volume of solution always being 5 ml. The flasks were then quickly attached to the manometric apparatus and the shaking mechanism started. It required 3–5 minutes for vapor pressure and temperature equilibrium to be established and the initial rapid changes in pressure to cease. The pressure reading at this time was taken as that for zero reaction. For reactions in pure oxygen, the gas was bubbled through water, filtered through glass wool, passed into the system through the stopcock at the top of the manometer and out through an outlet on the side of the reaction flask. Approximately 1/2 liter of gas was passed through the system in about five minutes.

The time lapse between preparation of the samples and actual observation of the change in oxygen pressure introduced an error not greater than 3%. This was checked by determining the Fe^{++} concentration by permanganate titration in such a solution three minutes after mixing.

All the glass joints were lubricated with Apiezon grease (M). Excess grease added to the reaction vessel did not affect the rate. It has been shown[2] previously that the reactions taking place in the Warburg reaction flasks are not diffusion controlled.

Results

Effect of Fe^{II} and Fe^{III} Concentrations.—The rate of oxidation is first order in ferrous iron concentration. This is evident from a study of the variation of initial rate with initial (Fe^{II}) at fixed phosphate and pyrophosphate concentration (Table I). Throughout this paper, M and F stand for mole liter^{-1} and formula wt. liter^{-1}, respectively. The molar concentrations of H_3PO_4, $H_2PO_4^-$, $H_3P_2O_7^-$ and $H_2P_2O_7^=$ in Table I are calculated assuming acid constants of 0.020 and 0.021 M for H_3PO_4 and $H_3P_2O_7^-$, respectively.

TABLE I

EFFECT OF Fe^{II} ON INITIAL REACTION RATE

$m = -d \ln(Fe^{II})/dt$ (hr.$^{-1}$), $(H^+) = 0.0177$ M, (H_3PO_4) = 0.188 M, ($H_2PO_4^-$) = 0.212 M, ($H_3P_2O_7^-$) = 0.0023 M, ($H_2P_2O_7^=$) = 0.0027 M, μ (ionic strength) = 1.0 − 1.1 M ($NaClO_4$), P_{O_2} = 151 mm., T = 30°

$(Fe^{II})_0$ (F)	0.003	0.010	0.020
m (hr.$^{-1}$)	.0789	.0772	.0800

It was not practicable to vary the Fe^{II} concentration over a larger range than that displayed in Table I. With lower concentrations, the manometer change due to reaction is small compared to fluctuations in the control (no Fe^{II}) runs. With higher concentrations, the reaction is too fast.

When $-\ln(Fe^{II})$ is plotted against t, fairly good straight lines (*cf.*, Fig. 1 of ref. 2) are obtained. At about 60% reaction, there was a decrease in slope of 10–20%. Usually at about 70% reaction, a white precipitate, believed to be ferric pyrophosphate, slowly formed. Addition of ferric ion initially produced the same phenomena immediately. Therefore, a detailed study of the kinetic effects of Fe^{III} addition did not appear to be profitable. Values for rate constants were taken from lines drawn through points up to about 40% reaction.

Effect of Phosphate Concentration.—In agreement with Cher and Davidson, we find that $-d \ln(Fe^{II})/dt = k_1(H_2PO_4^-)^2 P_{O_2}$. These results are given in Table II.

TABLE II

PHOSPHATE CATALYSIS OF THE Fe^{II}–O_2 REACTION

(30°, μ = 1.0 − 1.1 M, $NaClO_4$)

$(Fe^{II})_0$, M	(H_3PO_4), M	$(H_2PO_4^-)$, M	P_{O_2}, atm.	k_1, atm.$^{-1}$ M^{-2} hr.$^{-1}$
0.0100	0.200	0.200	0.198	4.00
.0100	.200	.200	.942	3.95
.0100	.415	.389	.198	3.96
.0100	.415	.389	.942	3.78
.0050	.415	.389	.198	3.64
.0050	.415	.389	.942	3.56
.010	.800	.200	.198	4.43

Av. k_1 = 3.90 (±0.22, mean error)

(3) J. Weiss, *Experientia*, **IX**, 61 (1953).
(4) O. Lanford and S. Kiehl, THIS JOURNAL, **64**, 292 (1942).
(5) T. Yamane and N. Davidson, unpublished work in this Laboratory.
(6) H. A. Spoehr, THIS JOURNAL, **46**, 1494 (1924).
(7) J. H. C. Smith and H. A. Spoehr, *ibid.*, **48**, 107 (1926).
(8) A. B. Lamb and L. W. Elder, *ibid.*, **53**, 137 (1931).
(9) R. E. Huffman and N. Davidson, *ibid.*, **78**, 4836 (1956).

The values of k_1 in Table II are generally somewhat lower (10–20%) than those reported by Cher and Davidson[2]; furthermore the ratio of rates in oxygen and air was close to the theoretical value of 4.8, whereas Cher and Davidson observed about 4.0. These differences probably are due partly to the use of redistilled water containing no Cu^{++} impurity in the present work, although it seems unlikely that this is the entire reason for the numerical discrepancy. The other causes however are unknown.

Effect of Pyrophosphate Concentration.—Pyrophosphate is an effective catalyst for the Fe^{II}–O_2 reaction. This is evident, for example, by noting that the rates recorded in Table I are about 5 times faster than predicted for phosphate catalysis alone.

Yost and Russell[10] quote values for the ionization constants of pyrophosphoric acid at 18° as follows: $K_1 = 0.14$, $K_2 = 0.011$, $K_3 = 2.1 \times 10^{-7}$, $K_4 = 4.06 \times 10^{-10}$; in 1 M KCl, $K_2 = 0.027$, $K_3 = 3 \times 10^{-6}$. The species present in significant amounts with $0.01 < (H^+) < 0.07$ are $H_3P_2O_7^-$ and $H_2P_2O_7^=$; it is accordingly necessary to determine a value of K_2 under the conditions of our experiments. This was done using a pH meter to measure the hydrogen ion concentration of solutions containing varying amounts of $H_3P_2O_7^-$ and $H_2P_2O_7^=$ at $\mu = 1.0$ ($NaClO_4$). A NaCl salt bridge was used because of the insolubility of $KClO_4$. The pH meter was calibrated to read 2.09 for 0.00814 M HCl in 1.00 M $NaClO_4$ at 30°. The results are shown in Table III. We have used $K_2 = 0.021$ M for the concentration ionization quotient of $H_3P_2O_7^-$ in interpreting the kinetic results (*cf.*, the discussion in footnote 13).

TABLE III

MEASUREMENT OF THE SECOND IONIZATION QUOTIENT OF PYROPHOSPHORIC ACID

($T = 30°$, $\mu = 1.0$ M, solutions prepared from standard HCl and $Na_4P_2O_7$ solutions.)

(H^+), M	$(H_3P_2O_7^-)$, M	$(H_2P_2O_7^=)$, M	K_2, M
0.00955	0.00874	0.00218	0.0239
.00912	.00918	.00213	.0212
.0126	.0118	.00187	.0200
.0120	.0124	.00180	.0176

The results of a set of runs in which $(H_2PO_4^-)$, $(H_3P_2O_7^-)$ and $(H_2P_2O_7^=)$ are all varied independently are exhibited in Table IV. These results show that the phosphate and pyrophosphate catalysis are independent and additive; and that the pyrophosphate catalysis is due principally to, and is first order in $H_2P_2O_7^=$; *i.e.*, that the rate law is $-\mathrm{d}\ln(Fe^{II})/dt = k_1'(H_2PO_4^-)^2 + k_2'(H_2P_2O_7^=)$ (in air, 30°). This result is demonstrated by the constancy of the calculated values of k_2', taking $k_1' = 0.794$ M^{-2} hr.$^{-1}$, with $(H_2PO_4^-)$ varied by a factor of 2, $(H_2P_2O_7^=)$ varied by a factor of 5.7, and $(H_3P_2O_7^-)/(H_2P_2O_7^=)$ varied by a factor of 3.8, all independently.

Unfortunately, a thoroughly satisfactory study of the effect of O_2 pressure on the pyrophosphate reaction path was not carried out. One series of runs was made at a time when difficulty with nonreproducible results was being encountered. This series gave ratios of rates in oxygen to rates in air of 3.7–4.3. The air results showed more scatter than the oxygen results. Comparison of the most consistent oxygen results obtained at this time with the consistent air results (Table IV) obtained later gives a ratio of 4.7 (±0.2). On this basis, it seems to us to be clear that the rate of the pyrophosphate catalyzed reaction is essentially proportional to the oxygen pressure and we write

$$-\mathrm{d}\ln(Fe^{++})/dt = k_1(H_2PO_4^-)^2P_{O_2} + k_2(H_2P_2O_7^=)P_{O_2}$$

(10) D. M. Yost and H. Russell, "Systematic Inorganic Chemistry," Prentice-Hall, Inc., New York, N. Y., 1946, p. 228.

TABLE IV

RATES IN THE PRESENCE OF PYROPHOSPHATE

$(Fe^{II})_0 = 0.010$ M, $T = 30°$, $\mu = 1.0$–1.1 M ($NaClO_4$)
$P_{O_2} = 151$ mm., $k'_1 = 0.793$ M^{-2} hr.$^{-1}$

(H^+), M	(H_3PO_4), M	$(H_2PO_4^-)$, M	$(H_2P_2O_7^-)$, M	$(H_2P_2O_7^=)$, M	k'_2, M^{-1} hr.$^{-1}$
0.0650	0.765	0.235	0.00945	0.00305	15.00
.0546	.732	.268	.01800	.00730	15.91
.0402	.667	.333	.03280	.01720	15.68
.0176	.188	.212	.00225	.00272	15.05
.0176	.377	.427	.00602	.00698	15.10
.0173	.373	.431	.00770	.00930	15.58
.0169	.369	.435	.00850	.01050	14.69
.0157	.176	.224	.00424	.00576	15.29

Av. $k_2' = 15.29$ (±0.33, mean error)

Effect of Surface.—Rate measurements in which Pyrex glass wool was added to the reaction flasks were performed in order to investigate possible surface catalytic effects. The surface area of the glass fibers[2] is estimated as 2300 cm.^{2} g.$^{-1}$. The surface area of the reaction flasks is about 50 cm.^{2}. Before introduction into the reaction flasks, the glass wool was heated to 500° in an oven for an hour, washed with hot aqua regia, rinsed copiously with water, dried and transferred to the cells. The results, presented in Table V, indicate that there is a negligible amount of surface reaction.

TABLE V

THE EFFECT OF SURFACE ON REACTION RATE

$m = -\mathrm{d}\ln(Fe^{++})/dt$ (hr.$^{-1}$), $\mu = 1.01$–1.1 M ($NaClO_4$), $T = 30°$, $P_{O_2} = 151$ mm.

(Fe^{++}), M	(H^+), M	$(H_2PO_4^-)$, M	$(H_2P_2O_7^=)$, M	Surface area, cm.^{2}	m, hr.$^{-1}$
0.020	0.020	0.200	0	50	0.0396
.020	.020	.200	0	985	.0264
.020	.0181	.210	0.00215	50	.0625
.020	.0181	.210	.00215	726	.0534
.020	.0165	.219	.00448	50	.1025
.020	.0165	.219	.00448	1007	.1040
.010	.0143	.234	.0083	50	.179
.010	.0143	.234	.0083	650	.200

Effect of Temperature.—A set of runs was performed at 20° in air at $(H^+) = 0.017$–0.024, with variable amounts of pyrophosphate. These results gave k_1' (air, 20°) = 0.25 (± 0.01) M^{-2} hr.$^{-1}$ and k_2' (air, 20°) = 10.70 (±1.0) M^{-1} hr.$^{-1}$. For this calculation, it is assumed that the ionization constant of $H_3P_2O_7^-$ does not change very much between 20 and 30°. It is known that K_1 and K_2 for H_3PO_4 do not change very much. The activation energies for the phosphate and pyrophosphate paths are calculated to be 21 (±1) and 6 (±1)

kcal. mole^{-1}. Cher and Davidson gave 20 (±2) for the former.

Discussion

We may summarize the results of the experiments with the rate law

$$-\mathrm{d}\ln(\mathrm{Fe}^{++})/\mathrm{d}t = k_1(\mathrm{H_2PO_4^-})^2P_{O_2} + k_2(\mathrm{H_2P_2O_7^-})P_{O_2} \quad \text{(a)}$$

with $k_1 = 3.90$ (±0.22 mean) atm.$^{-1}$ M^{-2} hr.$^{-1}$ (or $k_1 = 1.08$ (±0.06) × 10^{-3} atm. M^{-2} sec.$^{-1}$) and $k_2 = 76.8$ (±1.66) atm.$^{-1}$ M^{-1} hr.$^{-1}$ (or $k_2 = 2.13$ (±0.05) × 10^{-2} atm.$^{-1}$ M^{-1} sec.$^{-1}$) at 30° and activation energies of 21 (±1) and 6 (±1) kcal., respectively. Of course, the result does not mean that $H_3P_2O_7^-$ is not a catalyst; but the data indicate that it is less than, say, 10% as effective as $H_2P_2O_7^=$. Correspondingly, it is quite possible that catalytic effects due to $HP_2O_7^=$ would be significant at higher pH's where the concentration of this ion is larger.

The results show that the quadratic dependence on $(H_2PO_4^-)$ is not due to the equilibrium

$$2\mathrm{H_2PO_4^-} \rightleftharpoons \mathrm{H_2P_2O_7^-} + \mathrm{H_2O} \quad \text{(b)}$$

$$\frac{(\mathrm{H_2P_2O_7^-})}{(\mathrm{H_2PO_4^-})^2} = K_b$$

If such were the case, $K_b = k_1/k_2 = 0.051\ M^{-1}$. We shall now show that available thermodynamic data and reasonable estimates give $K_b = 6.8 \times 10^{-6}\ M^{-1}$ (with an uncertainty of a factor of perhaps 10–100). Therefore, the observed value of k_1/k_2 is too large by a factor of about 10^4.

For the reaction

$$\mathrm{H_2PO_4^-} + \mathrm{HPO_4^=} \longrightarrow \mathrm{HP_2O_7^=} + \mathrm{H_2O} \quad \text{(c)}$$

$\Delta H = 5810$ (± 130) cal. mole^{-1} [11] (in solutions with $\mu \sim 0.4\ M$ at 25°). From the empirical formula of Connick and Powell,[12] we estimate the entropy of $HP_2O_7^=$ as −5.4 e.u. and therefore, for reaction c, $\Delta S = -1.4$ (± 4, estimated) e.u. Therefore ΔF^0 (reaction c, 30°) = 6235 (± 1200), $K_c = 3.4 \times 10^{-5}\ M^{-1}$, uncertain by a factor of 7.5. The thermodynamic ionization constant of $H_2PO_4^-$ is 6.4×10^{-8}; at $\mu = 1$, we take $2 \times 10^{-7}\ M$. For the ionization constant of $H_2P_2O_7^=$ at $\mu = 1$ we take 1.0×10^{-6}.[13]

Therefore

$\mathrm{H_2PO_4^-} + \mathrm{HPO_4^=} = \mathrm{HP_2O_7^=} + \mathrm{H_2O}$	3.4×10^{-5}	(c)
$\mathrm{H_2PO_4^-} = \mathrm{HPO_4^-} + \mathrm{H^+}$	2×10^{-7}	
$\mathrm{H^+} + \mathrm{HP_2O_7^=} = \mathrm{H_2P_2O_7^-}$	1.0×10^{6}	

and adding, we get

$2\mathrm{H_2PO_4^-} = \mathrm{H_2P_2O_7^-} + \mathrm{H_2O}$	6.8×10^{-6}	(b)

It is very unlikely that this estimate is wrong by a factor of more than 10^2. It therefore is highly probable that k_1/k_2 does not equal K_b, *i.e.*, that the calculated ratio between them of 7.5×10^3 is not all due to experimental error and errors in estimates.

There are other arguments that discredit the hypothesis that the catalytic effect of phosphate is due to pyrophosphate maintained at equilibrium by reaction b. The hydrolysis of pyrophosphate is known to be too slow to maintain such an equilibrium,[14] but it can be imagined that there would be a catalytic effect of iron ions for reactions b. However, if such an equilibrium were maintained, the pyrophosphate added in our experiments would have hydrolyzed rapidly and almost completely, thereby increasing the phosphate concentration slightly and having an imperceptible effect on the rates.

The mechanism of the Fe^{II}–O_2 reaction for the case that the rate is first order in Fe^{II} and first order in O_2 has been discussed frequently before.[2,3,9] The two most attractive possibilities may be written schematically as

$$\mathrm{Fe^{II}} + \mathrm{O_2} \rightleftharpoons \mathrm{Fe^{III}} + \mathrm{HO_2} \quad (1,2)$$

$$\mathrm{Fe^{II}} + \mathrm{HO_2} \longrightarrow \mathrm{Fe^{III}} + \mathrm{H_2O_2} \quad (3)$$

$$\mathrm{Fe^{II}} + \mathrm{H_2O_2} \longrightarrow \text{further oxidation (fast)} \quad (4)$$

or

$$\mathrm{Fe_{II}} + \mathrm{O_2} \rightleftharpoons \mathrm{Fe^{IV}} + \mathrm{H_2O_2} \quad (5,6)$$

$$\mathrm{Fe^{II}} + \mathrm{H_2O_2} \longrightarrow \text{further oxidation} \quad (4)$$

There is at present no compelling reason for favoring one path or the other. The occurrence of the first scheme would be proved by observing inhibition by Fe^{III}, corresponding to competition between reactions 2 and 3. In the present case it was not practicable to search for such an effect because of the formation of complex ions and insoluble solids containing Fe^{III} and pyrophosphate.

Pyrophosphate is a good complexing agent for Fe^{III} and undoubtedly also for Fe^{IV}. Its catalytic effectiveness probably is due to the stabilization of the transition state for reaction 1 or reaction 5 by complexing the iron ion in the transition state molecule, as suggested by Weiss. As pointed out previously,[9] there is a correlation between the complexing affinity of an anion X^- for Fe^{III} and its catalytic effectiveness in the bimolecular Fe^{II}–O_2 reaction.

PASADENA, CALIFORNIA

(11) J. M. Sturtevant and N. S. Ging, THIS JOURNAL, **76**, 2087 (1954).

(12) R. E. Connick and R. E. Powell, *J. Chem. Phys.*, **21**, 2206 (1953). We are indebted to Professors Connick and Powell for correspondence concerning this matter.

(13) S. M. Lambert and J. I. Watters, THIS JOURNAL, **79**, 4262 (1957), give 7.6×10^{-7} for the quantity $[H^+](HP_2O_7^=)/(H_2P_2O_7^-)$ at $\mu = 1((CH_3)_4NCl)$ at 25°, where brackets and parentheses indicate activities and concentrations, respectively. We estimate $\gamma_H = 0.76$, so that the concentration equilibrium constant is $1.0 \times 10^{-6}\ M$. These authors give $[H^+](H_2P_2O_7^=)/(H_3P_2O_7^-) = 6.0 \times 10^{-4}$ at $\mu = 0.1$ at 25°, from which we estimate $K_2 = 8 \times 10^{-4}\ M$ at $\mu = 0.1$ and 25°. This is to be compared with the value 0.021 M at $\mu = 1.0$ and 30° which we have used (*cf.* Table III).

(14) D. O. Campbell and M. L. Kilpatrick, *ibid.*, **76**, 893 (1954).

PROPOSITIONS

1. Preliminary investigations, reported in this thesis, of the fluoride resonance in HF solutions containing ferric ions indicated an unexplained behavior of the resonance line. As the ferric ion concentration is increased in the solution, the amplitude of the resonance line was found to decrease. This behavior could also be induced by heating the sample. It is highly probable that some type of chemical exchange is responsible for the observed phenomenon, although there was no perceptible broadening or shift of the line. It would be of interest to study this effect as a function of pH, since it was not found in the NH_4F solutions containing ferric ions.

2. An EPR investigation of the cobaltous cyanide complex ($CoCN_6^{-4}$) is proposed (1).

3. Evidence has been reported which indicates that the fluoride relaxation times, $\underline{T}_1$ and $\underline{T}_2$, are not equal in aqueous potassium fluoride solutions (2). It is proposed that a study of the system, using mixtures of D_2O and H_2O, be undertaken in order to ascertain the role of the solvent protons in producing this anomaly.

4. It is proposed that the Fe^{II} - Fe^{III} electron exchange reaction be investigated in solutions containing high concentrations of ammonium fluoride. In such a system, it has been shown that the predominant complex is the $FeF_6^{\equiv}$ ion (3).

5. It is proposed that a study be made of the relaxation times of O^{17} in aqueous solutions of vanadyl sulfate in order to

see whether the anomalous T_1/T_2 ratio found in Mn^{++} solutions (4), also exists in this system.

6. A determination of the rate of the reaction (5) using the technique

$$I^{*-} + ICN \rightleftarrows I^{*}CN + I^{-}$$

of NMR is proposed.

7. Since ferrihemoglobin is found to be essentially dissociated around a pH of 11 (6), an extension, to high pH's, of the work of Davidson and Gold (7) on the relaxation time of water protons in ferrihemoglobin solutions should give added information as to the position of the iron atoms in the molecule.

8. A magnetic resonance investigation of the paramagnetic species formed by the action of ozone on strongly acidified silver nitrate solutions (8), is proposed. The existence of Ag^{+2} and/or Ag^{+3} in the system could be established, and the rate of electron exchange in the system could be studied.

9. An investigation of the reaction between iodine monobromide and triethylsilane is proposed. Since it is believed from studies of the reactions of triethylsilane that the hydrogen attached to the silicon is highly electronegative (9), (10), (11), (12), such an investigation should yield information as to the mechanism of the halogenation reactions of triethylsilane. Using IBr, it would be of interest to see whether bromination or iodination occurs. Such a study might also aid in understanding the anomalous addition of IBr to phenols and related compounds (13), (14), (15).

10. Arrangements should be made by which graduate students are allowed to use other facilities, when it becomes

impossible for them to work in their assigned rooms due to the necessary construction work taking place.

REFERENCES TO PROPOSITIONS

1. W. Latimer and J. Hildebrand, Ref. Book of Inorganic Chem. (MacMillan Co., New York, 1953) p. 426.
2. I. Solomon and N. Bloembergen, J. Chem. Phys., 27, 572 (1957).
3. Section III of Part I of this thesis.
4. Section II of Part I of this thesis.
5. F. Jenkins and G. Harris, J.P.C., 61, 249 (1957).
6. Private communication from William D. Hutchinson.
7. N. Davidson and R. Gold, Biochimica et Biophysica Acta, 26, 370 (1957).
8. A. A. Noyes, K. S. Pitzer and C. L. Dunn, J.A.C.S., 57, 1229 (1935).
9. J. Jenkins and H. Post, J. Org. Chem., 15, 556 (1950).
10. F. Price, J.A.C.S., 69, 2600 (1947).
11. H. Westermark, Acta Chem. Scand., 8, 1086 (1954).
12. F. Whitmore, E. Pietrusza, and L. Sommer, J.A.C.S., 69, 2108 (1947).
13. A. Sharpe, J. Chem. Soc., 4, 3713 (1953).
14. D. Pearson, and C. Ross, J.A.C.S., 74, 2933 (1952).
15. F. Bennett, and A. Sharpe, J. Chem. Soc., 2, 1383 (1950).